
**EXPLORATORY DATA ANALYSIS
OF
ALS PATIENT DATA**

A CASE-STUDY OF COGNITIVE DATA FROM A PATIENT WITH
AMYOTROPHIC LATERAL SCLEROSIS

Minerva Schools at KGI

Capstone Project

AUTHOR:

Michelle Hackl

SUPERVISORS:

Professor T. Stan

Professor M. Grosse-Wentrup

IN COLLABORATION WITH:

Research Group for Neuroinformatics,
University of Vienna

Institute for Psychology,
University of Würzburg

1 Abstract

In this project, I present a concise overview of past attempts at brain-computer interface (BCI) communication with Amyotrophic lateral sclerosis (ALS) patients and some of the hypotheses about why they have been unsuccessful to date. This project is an exploratory data analysis of 86 hours of current EEG data collected from a CLIS (completely locked-in state) ALS patient. The analysis aims to extract cognitive activity in different frequency bands and observing their change over time. The goal of this is to identify cognitive measures that are stable enough to facilitate the identification of "high interest/high alertness" periods during which BCI communication with the patient is more likely to succeed.

The analysis suggests that the Dreem headset provides sufficient data quality for long-term recordings (little low-frequency noise and limited artifacts). We were able to identify two distinct frequency bands in the 1-2.5Hz and 2.5-4.5Hz ranges. Analysis results suggest a significant, positive correlation between this "alpha" and "theta" activation despite outlier and total power corrections. Potential explanations for this observation are provided. A follow-up experiment (currently in progress) is described.

1	Abstract	1
2	Literature Review	4
2.1	Intro to Amyotrophic Lateral Sclerosis	4
2.2	LIS and the Transition to CLIS.....	5
2.3	BCI in ALS Patients.....	6
2.4	Frequency Bands	7
2.5	Relevance to ALS & Subject Heterogeneity	9
2.6	Thought Extinction Hypothesis	10
2.7	Alternative Hypothesis	11
2.8	Summary.....	13
3	Hypothesis Section.....	14
3.1	Research Questions.....	14
3.1.1	Experiment 1.....	14
3.1.2	Experiment 2.....	16
4	Methodology	18
4.1	Experimental Timeline.....	18
4.2	Recording Setup	20
4.2.1	Basic Setup - Dreem	20
4.2.2	Auditory Stimulation Setup	22
4.3	Data Collection	28
4.3.1	Experiment 1.....	28
4.3.2	Experiment 2 - Auditory Stimulation	29
4.4	Data Preprocessing	29
4.4.1	Dreem Preprocessing	30
4.4.2	Basic Preprocessing	30
4.4.3	Visualizing the Data.....	31

4.4.4	Data Annotation	31
4.4.5	Feature Extraction	36
4.5	Data Analysis Methods Overview.....	36
5	Results	38
5.1	Data Quality of the Dreem Headset	39
5.2	Calculating Significance	42
5.3	Describing Covariance	43
5.3.1	Within-band Covariance	43
5.3.2	Frequency Covariance	46
5.3.3	Amplitude Covariance.....	47
5.3.4	Amplitude - Outlier Corrected.....	48
5.3.5	Amplitude - Power & Outlier Corrected.....	49
5.4	Amplitude and Frequency Over Time	51
5.4.1	Changes in Frequency	51
5.4.2	Changes in Alpha Over All Recordings.....	52
6	Discussion and Conclusions	54
7	Glossary	56
8	Bibliography	58
9	Appendix	62
9.1	Code for Inter-Stimuli Wait-times.....	62
9.2	Auditory Stimulation Parameter Test	64
9.3	Code Notebooks	65
9.4	IRB	65

2 Literature Review

This paper provides a general overview of Amyotrophic lateral sclerosis (ALS) and aims to guide the reader through the existing literature on brain-computer interface research for that patient group. As of the writing of this paper, research has yet to establish reliable communication for late-stage patients once they enter a fully paralyzed state. This group is most in need of the ability to communicate. I present an extensive analysis of a late-stage ALS patient's cognitive data in the hopes of identifying a reliable signal that could be utilized to establish communication at opportune times. The literature review provides an overview of the disease and its progression, patient's cognitive states, existing BCI research, and connected concepts as well as the two most prominent hypotheses for why communication has failed to-date.

2.1 Intro to Amyotrophic Lateral Sclerosis

What is Amyotrophic Lateral Sclerosis?

Amyotrophic lateral sclerosis (ALS) is a rare (prevalence: 5.2 per 100.000) and fatal neurodegenerative disease characterized by motor neuron degeneration in the spinal cord, brainstem, corticospinal tract, and the primary motor cortex. The neuron degeneration leads to progressive muscular paralysis (Wijesekera & Leigh, 2009).

Two-thirds of patients have limb onset ALS, starting either proximally or distally in the upper and lower limbs, one third are bulbar onset cases, affecting the corticobulbar tract with symptoms affecting facial muscle control and gaze first. Muscle paralysis progresses until a locked-in state (patients are entirely unresponsive due to loss of voluntary muscle control) and eventually leads to death due to respiratory failure, after an average of 2-3 years for bulbar onset and slightly longer for limb onset ALS (Wijesekera & Leigh, 2009).

The exact causes of ALS are unknown, and it is commonly accepted that ALS has complex genetic-environmental interaction factors (Shaw, 2005; Cozzolino, Ferri & Carri, 2008). Some factors identified by Rocha et al. (2005) are genetics, auto-immunity, oxidative stress, glutamate excitotoxicity, and abnormal neurofilament aggregation. No consistent hereditary factors have been identified so far (Hackl, 2018; unpublished).

While ALS is first and foremost considered a motor-neuron disease, the accompanying cognitive impairments have been researched for more than two decades now (see Massman & Appel, 1996; for an early-stage testing battery). As Neumann & Kotchoubey (2004) point out, most cognitive tests rely on fast motor responses, either verbal or manual, and hence are unfit to test the cognitive state of motor-impaired patient groups such as ALS. They instead proposed a battery of tests that relied on binary answers with no speed component or that are entirely EEG based for late-stage patients. Such tests have been implied in researching cognitive impairments in ALS patients, concluding varying degrees of impairment. Older studies found anywhere from 1% to 70% of patients having some form of cognitive impairment, suggesting sample heterogeneity (Brownell et al., 1970; Frank et al., 1997). Recent research found converging evidence for around 50% of ALS patients having moderate to severe cognitive impairments (see Ringholz, 2005; for a summary of related studies). The relation between disease severity, duration, and impairment, however, is not as clear as would be expected, and research into the cognitive states of completely locked-in patients is sparse and inconclusive (see below).

2.2 LIS and the Transition to CLIS

What aspects of ALS do I care most about and why?

Patients' communication ability is usually unaffected with the onset of the disease, but the gradual muscle paralysis tends to make it more and more difficult to communicate over time. Along the deterioration of communicative capacity, there are two recognized states: "locked-in" state (LIS), characterized by complete paralysis with remaining voluntary eye movement or minimal facial muscle control (Kübler & Birbaumer, 2008). For this stage of the disease, eye-tracker spellers are available that aid the patients in writing or navigating the web and maintaining some degree of autonomy (Polido et al., 2014; Polido et al., 2015). Once voluntary eye movement control ceases, patients are described to be in a "completely locked-in" state (CLIS). Because of the current inability to generate reliable BCI systems for this late disease stage (reviewed below), patients lose their ability to communicate and hence all remaining autonomy over their lives. **The goal of the continued research in this area is to develop a reliable method of BCI communication that can accompany patients as they transition from locked-in to completely locked-in state.**

2.3 BCI in ALS Patients

What have we tried? Why is communication with CLIS patients difficult?

With this goal in mind, Murguialday et al. (2011) conducted a study aimed at better characterizing the transition from LIS to CLIS state with respect to cortical and physiological changes. They recorded several different signal sources (electromyography from facial muscles and the external anal sphincter, electrooculographic and electrocorticographic), testing what they believed to be potentially still responsive muscles and senses in late-stage patients and the corresponding cognitive signals. The performed motor imagery tasks and visual stimulation elicited no significant response, while tactile stimulation showed some reactivity only in muscle joint receptors. Only auditory stimulation seemed largely intact and preserved across the transition from LIS to the CLI stage.

Since the most commonly used paradigms for BCIs are unavailable in late-stage ALS patients (motor control ceases together with tactile and visual responses), auditory stimulation remains as the most promising method of establishing BCI communication for those patients. Kim et al. (2012) present several auditory paradigms that could be utilized for this, based on either slow cortical potentials, event-related potentials (ERP), or selective attention and spatial hearing. As of now, these methods are slow and ineffective in communicating, since information has to be presented consecutively and one bite at a time, leading to a rather slow information transmission rate only feasible for a simple yes/no communication (Kübler & Birbaumer, 2008; Laureys, Gosseries, & Tononi, 2009). Nijboer et al. (2008) have successfully utilized an ERP-based speller to establish continued communication with a patient approaching a completely locked-in state.

Despite such minor successes in identifying intact auditory pathways as an approach to BCI communication, the researchers also note that attempts at utilizing this knowledge to establish auditory BCI in CLIS patients reliably have been futile so far (Murguialday et al., 2011). Meta-studies confirm that the classification accuracy achieved in completely paralyzed ALS patients does not differ from chance level (Marchetti & Priftis, 2015). Similarly, attempts at BCI communication have been made using slow cortical potential, motor imagery, P300-based systems, and semantic conditioning (see Grosse-Wentrup, 2019 for detailed review), all ultimately unsuccessful in establishing reliable communication with CLIS patients.

As such, the transition from LIS to CLIS in patients is not only marked by loss of motor control, visual reactivity and tactile senses but also marks the point at which BCI communication with the patient seems to become impossible (Kübler & Birbaumer, 2008). Hypotheses as to why this is the case have been established and are presented below.

2.4 Frequency Bands

What are the cognitive frequencies we utilize for BCI communication?

There are two popular methods for controlling BCI systems using EEG, generally classified as *active* and *passive* BCI. Passive systems use external triggers (i.e., flashing lights or sounds) and read out the brain's passive response to the stimulus and active systems consist of those where patients learn to modulate their brain's activation directly to control the BCI system.

In both active and passive BCI systems, the most common methodology for supporting response classification to a question is to look at different frequency band modulations or changes in their amplitude (these could be actively modulated by patients or passively observed in response to external stimuli). Increased activation in specific frequency bands is achieved when large neuronal populations oscillate in synchrony, an ability that most likely serves the brain's integrative ability (Başar et al., 2001). My research, in particular, looks at long-term changes in those frequency bands and how they might affect what we know about a patient's cognitive state. This review is focused on Alpha, Theta, and Delta bands, as they are most relevant to the results presented below. For a more detailed review of other bands, check the review by Başar et al. (2001).

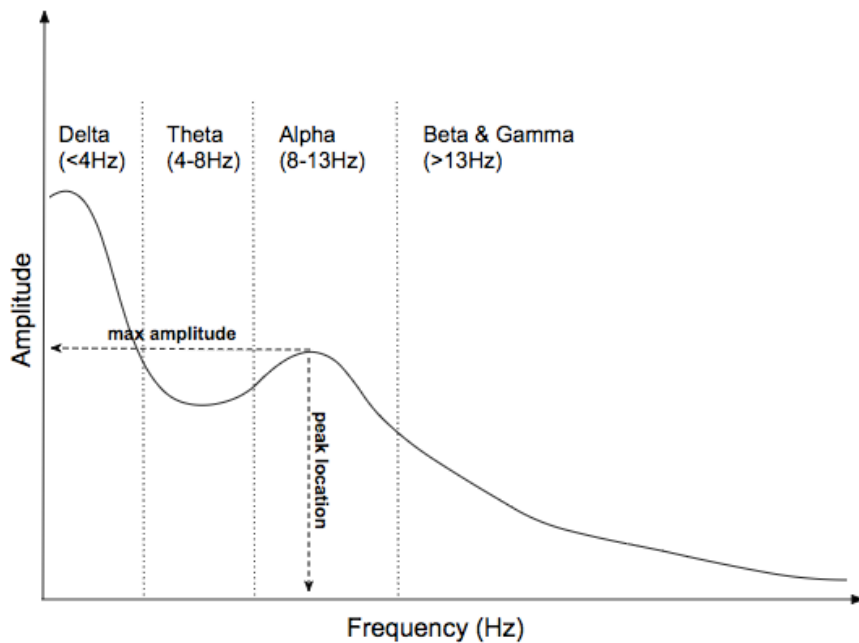


Figure 1. What a common resting-state amplitude-frequency plot of a healthy patient might look like. The frequency bands are denoted with their most common measures of max amplitude and peak frequency location in a particular frequency band.

Alpha - Alpha rhythms have commonly been linked to cognitive performance in a number of tasks and, because they are the most easily distinguishable, are often used for BCI systems. Relaxation, sleep states, and sedative drugs tend to up-regulate alpha activity (higher amplitude), while cognitively demanding tasks will suppress alpha peaks. Most individuals have a somewhat steady alpha peak location, varying locally by about $\pm 0.5\text{Hz}$ (Kiloh et al., 1972; Niedermeyer & da Silva, 2005), and that can vary significantly with age (Wilkinson & Allison, 1989). Long-term, higher alpha peak location is positively correlated with good cognitive performance, and larger amplitude variance between resting and non-resting states is similarly correlated with good cognitive and memory performance (Klimesch, 1999).

Theta - Theta band changes are inversely related to alpha rhythms. Where large overall alpha amplitude indicates good cognitive and memory performance, the corresponding low amplitude in theta indicates the same. Research has found

that while slow-wave activation will decrease with age, a higher absolute theta will correlate with increased performance measures (Vlahou et al., 2014; see Finnigan & Robertson, 2011 for similar results for relative theta activation). During most task performance, theta up-regulates while alpha down-regulates (Klimesch, 1999). In particular, working memory tasks have been linked to this desynced oscillatory behavior (Sauseng et al., 2005). Drug-induced changes in this range have also shown effects on learning and LTM (animal model) (Givens & Olton, 1995; Stäubli & Xu, 1995).

Delta - Commonly associated with deep sleep stages. Less commonly used in BCI classification, as low-frequency bands are easily affected by EEG artifacts (e.g., eye movement) and most BCI signal cleaning methods are tailored to higher frequency bands (Wang et al., 2009).

2.5 Relevance to ALS & Subject Heterogeneity

How is alpha peak frequency related to cognitive impairment? How does it vary across patients?

As has been discussed in previous sections, ALS is a rather heterogeneous disease in several aspects, in particular when it comes to cognitive profiles. Ringholz's meta-analysis of cognitive impairment in ALS patients (2005) clearly shows that disease progression and cognitive impairment are only weakly correlated, and they denote that substantial heterogeneity was observed in most studies. Klimesch (1999) additionally noted that alpha peak frequency should be determined for each subject individually, as inter-subject variability is less indicative of performance. Despite its variability, alpha peak frequency has clearly been linked to cognitive performance in correlational studies in humans, and evidence suggests a causal link between the two from animal models (Givens & Olton, 1995; Stäubli & Xu, 1995). As described, higher alpha peak frequency, as well as increased alpha-theta regulation (this would show as a strong negative correlation between the two), are associated with heightened cognitive states.

As such, researchers have focused on better understanding alpha peak variance within subjects, as an indicator of cognitive performance. Hohmann et al. (2018) have focused efforts on classifying alpha rhythm changes in late-stage patients. Using topographies of the identified frequency peak signals, they demonstrated that in one LIS patient, what appears to be an alpha rhythm, had dropped as low as 3.8Hz, with significant variational patterns over the course of a 10-hour recording (Konieczny, 2019; unpublished). Signorio et al. (1995) found

similar results in patients with Alzheimer's, noting that 44% of their patients lacked a normal alpha activation, but showed heightened activation in the 1-6.5Hz range. Identifying the peak signal to be alpha in this manner is correlational evidence for the down-shift hypothesis. The second experiment presented here aims to extend upon these findings with causal evidence. Overall, these findings encourage research into the connection between cortical rhythm changes and cognitive performance and, by extension, BCI communication abilities.

2.6 Thought Extinction Hypothesis

Why are we unable to communicate with CLIS patients?

From the failings to establish communication with CLIS patients, the research shows a current effort to better understand this CLIS and the cognitive implications of moving from a LIS to complete locked-in-ness. In their correlational meta-analysis of 29 ALS patients, Kübler & Birbaumer (2008) proposed the "thought extinction hypothesis", hypothesizing that the inability to communicate effectively with the outside world leads to gradual extinction of goal-directed thinking (see Figure 2).

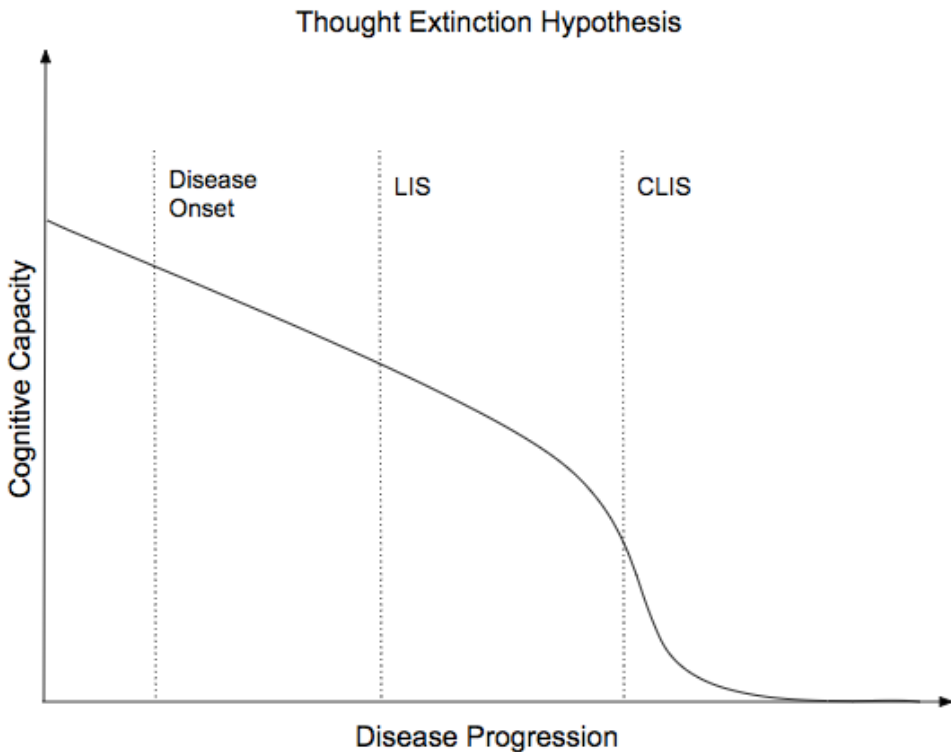


Figure 2. Visualization of the Thought Extinction Hypothesis. Cognitive capacity declines gradually until a completely locked-in state is reached, at which point cognitive capacity declines rapidly with the inability to interact with the outside world.

No follow-up experiments in support of this hypothesis have been performed so far (current as of 2020). A study in LIS patients by Ringholz et al. (2005), however, found no significant correlation between cognitive impairments and the severity or duration of patient symptoms. This suggests that the worsening of symptoms might, at the very least, not be a clear indication of a patient's cognitive state and provides mild counter-evidence to the hypothesis of an overall, gradual thought extinction.

2.7 Alternative Hypothesis

What alternative hypotheses exist?

The authors of this paper did not perform their experiments under the assumption of the thought extinction hypothesis being the primary explanation for the observed inability to communicate with patients. While we acknowledge the evidence for gradual cognitive decline in ALS patients (Ringholz, 2005), we

believe the inter-subject variability is too large to draw general conclusions from the observed evidence. Instead, we hypothesize that, despite the cognitive decline, some patients might retain their ability to communicate into late-stage disease progression, but because of a lack of communication interface and opportunity, will not be inclined to or capable of clear communication for the most time. We hypothesize that there may be short (or long) time-windows of higher cognitive activity throughout the day, during which patients could reliably be asked to communicate and that such time-windows could be found using reliably identifiable cognitive signals (see Figure 3 for a visualization of this hypothesis). The exploratory data analysis performed here is structured around searching for and quantifying such signal patterns, if they exist, in the hopes of utilizing them to identify opportune times for establishing BCI communication.

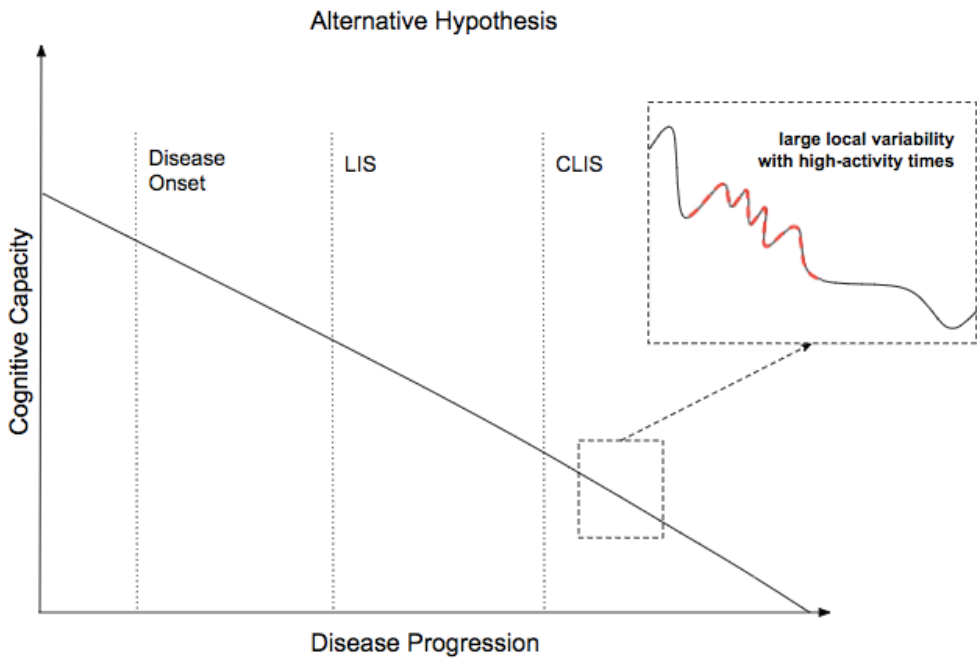


Figure 3. Alternative hypothesis visualized. Cognitive decline is gradual past the CLIS state, but local variability increases and high-activity times, during which BCI communication would be possible, become rarer. Figure inspired by lecture notes from Prof. Grosse-Wentrup.

2.8 Summary

In this literature review, I have presented a review of Amyotrophic lateral sclerosis and the associated disease stages. I have reviewed evidence for the potential to establish BCI communication with late-stage patients as well as the current inability to do so reliably. I review evidence for why I consider a detailed investigation into cognitive states of this patient group worthwhile and reviewed the currently most prominent hypotheses for how disease progression affects patients' general cognitive state as well as the ability to communicate using BCI. In the following sections, I present the guiding questions for my research and the resulting hypotheses that this paper is investigating.

3 Hypothesis Section

From the above review of the existing literature on ALS, the observed individual differences in cognitive patterns between patients and in particular attempts at BCI communication with LIS and CLIS patients, there emerges a need for a better understanding of the patients' cognitive states and intra-subject variability, in the hopes of being able to communicate with CLIS patients. In the following section, I review the questions and hypotheses the two conducted experiments aim to answer and explore.

All aspects of the data analysis are aimed at two fundamental goals: Primarily, more clearly understanding what consistent measures of brain activity exist for patient LEK, and how they vary with respect to one another over time. Secondarily, better describing the patient's cognitive neuronal oscillation changes as their disease progresses, which is possible with the current data set, since extensive recordings were performed over a period of several months. All in the hopes of being able to identify a potential signal to search for a measure of "alertness" during which the patient might best be able to communicate via BCI.

3.1 Research Questions

3.1.1 Experiment 1

The first experiment performs an extended data analysis on 87 hours of CLIS patient data (Konieczny, 2019; unpublished). Its goal is to investigate the patient's neuronal oscillation patterns to identify a robust measure that could potentially be investigated for signs of cognitive alertness. Firstly, it tries to establish if the used recording equipment is capable of identifying cognitive signals well enough:

- Does the Dreem headset (see 5.3.1 for a detailed description of the data collection setup) provide sufficient data quality to reliably extract cognitive signals of neuronal oscillation (in particular in the 1-50Hz range) over time?

After establishing sufficient signal quality to extract measures of interest, the experiment searches them for patterns of covariance or time-based correlation. I identify two consistent signals in the 1.5-4.5 Hz frequency range and analyze them to answer the following questions:

- How do the amplitude and frequency of the identified bands vary over time (measured in months/ over the course of a day)?
- How do the different bands vary in relation to one another (over time/ over a day)?

As discussed in the literature review, I expect the patient's traditional "alpha" signal (used to identify cognitive ability in healthy patients) to be shifted toward the lower frequency bands. Hence:

- If one of the observed signals in the 1.5-4.5 Hz range could be identified to be a down-shifted "alpha" how does its variability change over time/ with the time of day?

These questions will guide the data exploration. The implicit hypotheses underlying them are stated below, together with the assumptions and observed evidence they are based on:

- **H1:** There is a gradual reduction in mean "alpha" frequency over time.

This hypothesis is supported by the evidence described in the literature review of having observed a down-shifted "alpha" pattern in this very patient in past recordings (Hohmann et al., 2018). The underlying assumption made here is that the trend of gradual reduction continues smoothly over time, leading us to believe the now highest activation band in the 2.5-4.5 Hz range is "alpha". It is possible that the reduction is not gradual, however, and an alternative hypothesis would be that activation in the "alpha" frequency is simply extinct, with the observed activations being more traditional low-frequency activations, such as theta or delta, common during deep sleep stages (Wang et al., 2009). Experiment 2 further explores evidence to support **H1**.

- **H2:** Interesting patterns of co-variation between peak amplitude and frequency of different bands exist over time, as well as throughout the course of a day.

As described, patterns of amplitude and frequency variations in different frequency bands have been identified to correlate with a number of cognitive states and abilities (Sauseng et al., 2005). I expect similar patterns to emerge in the data of this study, based on the assumption that some or all of the relations between the frequency bands continue to exist in CLIS patients. While we can

use LIS patient data to support this, for CLIS patients, this assumption is necessarily somewhat cyclical. If reliable patterns exist and could be utilized to communicate with patients, then we could prove that such patterns exist and can be utilized to communicate with patients. I take this assumption on good faith, hoping that an eventual success in communicating with CLIS ALS patients will prove the assumption.

- **H3:** Identifying such patterns would allow identifying "high interest" times throughout the day during which BCI communication might be more likely to succeed.

The performed data analysis and followup experiment are aimed at laying the groundwork for **H3**. I hope that my work will support future researchers in identifying potential "high alertness" times throughout the day and eventually establish communication with CLIS patients.

3.1.2 Experiment 2

The second experiment, conducted as a follow-up to experiment 1, is specifically aimed at investigating the "alpha" frequency we identified in experiment 1. Since the frequency peaks of our ALS patient are in much lower frequency ranges (2.5-4.5 Hz) than in healthy patients (8-13Hz), it is difficult to claim that this is, in fact, a shifted alpha peak without further evidence. The second experiment investigates the peak-shift hypothesis, building on the described findings by Hohmann et al. (2018):

- **H4:** The peak frequency observed in the 2.5-4.5Hz range is a down-shifted alpha peak.

Alternative hypothesis:

- Alpha activation is extinct in our CLIS patient, and the observed activation in the 2.5-4.5Hz range is a "traditional" delta or theta activation pattern.

To identify whether the peak frequency observed is a down-shifted alpha activation, the second experiment assumes that, if it behaves similarly to a traditional alpha peak, this constitutes supporting evidence in favor of it "being" a down-shifted alpha. To test this hypothesis, the second experiment is interventional in nature and performs auditory stimulation during recording,

which is known to yield P300 amplitude decreases in healthy patients (Laureys, Gosseries, & Tononi, 2009). To observe supporting evidence for **H4**, we would want to see a similar P300 decrease in the 2.5-4.5Hz range in response to the presented stimuli. Such a result would provide support to both the results presented in this experiment as well as past efforts such as by Hohmann et al. (2018).

4 Methodology

In the following, I present the experimental timeline of the two experiments as well as the technical setup for both of them, in particular the stimulation setup for experiment 2, which was constructed for this experiment from scratch. I then present details on the data collection and stimulation parameters as well as specific preprocessing and data annotation steps for removing artifacts and extracting features for the analysis.

4.1 Experimental Timeline

As referred to throughout this paper, data for experiment 1 was collected prior to the start of this project back in 2018. Upon initial analysis of the data, we found interestingly little activity in the traditional alpha-range, but an "alpha-looking" peak in a lower frequency range. From this, we generated the hypothesis for experiment 2. For this follow-up experiment, we designed and built a stimulation setup, which is currently being used by the University of Würzburg to collect follow-up data. Analysis of the data collected by the University and continued analysis of the original dataset were performed side-by-side with the other aspects of the project.

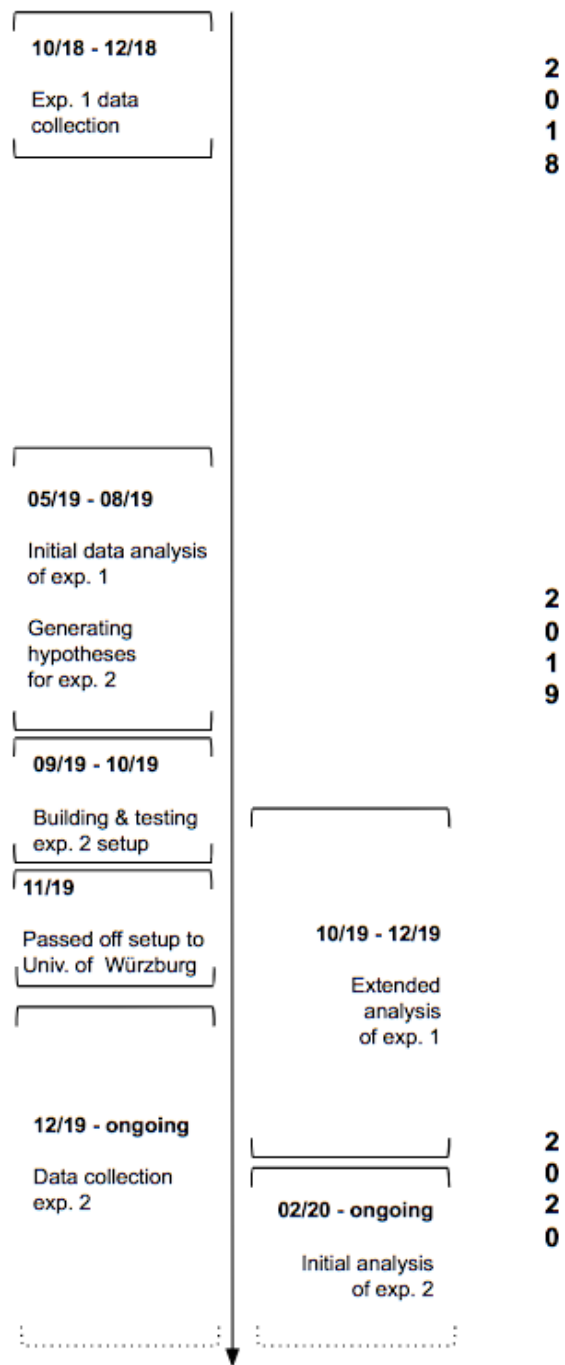


Figure 4. Experimental timeline detailing data collection and analysis workflows for experiment 1 & 2.

4.2 Recording Setup

4.2.1 Basic Setup - Dreem

All data was collected using the Dreem EEG headset, a low-cost, 5-electrode EEG system initially aimed at sleep-stage classification and deep sleep stimulation for enhanced sleep quality. Disabling the deep-sleep stimulation feature through the app, allowed us to use the device as a conventional EEG system for long-term recordings. Since the headset is configured to be worn during sleep, it is noticeably more comfortable than conventional EEG systems and can easily be worn for its full recording length (up to 12 hours). Electrode positions are indicated in Figure 5.

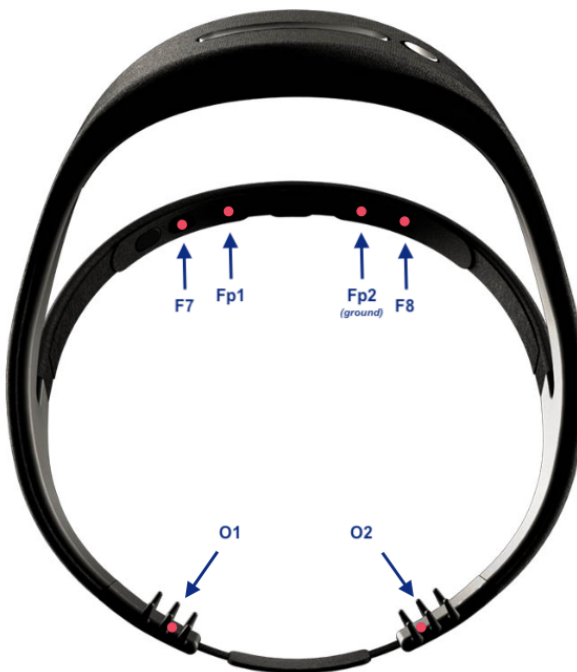


Figure 5. Electrode positions of the Dreem 2 headset. F7, Fp1, Fp2, and F8 are located on the forehead, with Fp2 serving as the ground. O1 and O2 are located on the back of the device, lying against the occipital bone during recordings.

Electrodes are referenced to seven numbered channels by the Dreem headset, which correspond to the following channels in order: 'Fp1-O1', 'Fp1-O2', 'Fp1-

'F7', 'F8-F7', 'F7-O1', 'F8-O2', 'Fp1-F8'. 'O1-O2' is generated in the data preprocessing step.

We visited patients in their private homes for the recordings and aided their caretakers in placing the fully charged headset on the patient. The researcher then started the recording session through the app, and caretakers were instructed on how to ensure continued data quality after moving the patient (i.e., if they moved the patient from their wheelchair to a bed, the caretaker was instructed to check for suitable electrode-skin connectivity afterward). Caretakers left the patients with the headset for as long as it was convenient (instructions for up to 12 hours) and were instructed to remove the headset afterward. The headset tracks if it is being worn through a pressure button, and will turn off automatically after 1 hour if it is not being worn. This "turn-off" period is visible on the recordings. The researcher later collected the headset, reconnected it to wifi, and uploaded the collected data to the dreem-viewer platform.

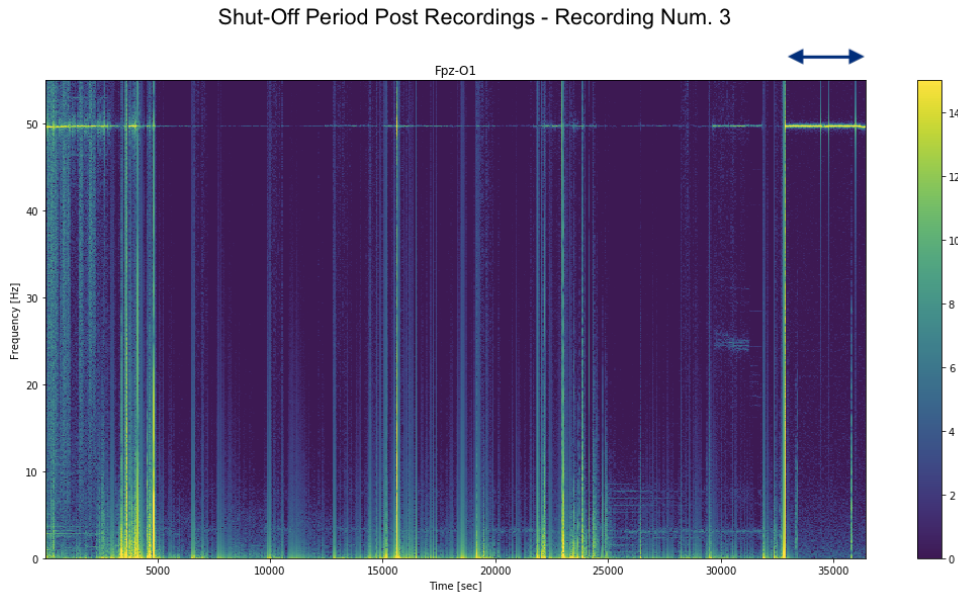


Figure 6. One hour-long period after taking off the headset before the recording ends automatically, as indicated by blue arrows above the plot. It is clearly visible across all channels of the recording, often separated from the rest of the recording by a short period of noisy data (generated by taking off and moving the headset).

4.2.2 Auditory Stimulation Setup

For the second experiment, we wanted to perform auditory stimulation of patients to test if the observed “alpha” peak frequency would react as expected. To perform auditory stimulation, we needed to combine an external device for stimulation with the Dreem recording setup. For its size and ease of use, a Raspberry Pi (Model 3+) was chosen to perform this auditory stimulation during recordings. A Raspberry Pi with an adequate battery pack can be operated independently from a power socket for up to 12 hours and hence can be connected to the Dreem headset and moved around with the patient comfortably. The goal was to keep the ease of use of the recording setup high for caretakers, despite adding additional hardware. The Pi was carefully packaged to prevent damage to the hardware during recording sessions. Figure 7 illustrates the packaging, Figure 8, the dimensions of the additional hardware.



Figure 7. Packaging for Raspberry Pi allowing for easy access to all needed ports, while preventing movement in the box, such that the hardware cannot be easily damaged during recordings.

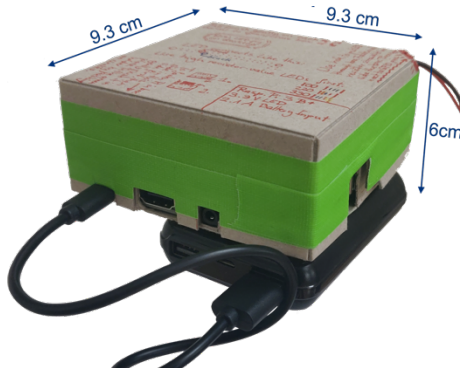


Figure 8. Dimensions for Pi and battery pack. 9.3 x 9.3 x 6 cm.

While being convenient for long-term recordings, the Dreem is not equipped with functionalities that traditional research headset have (i.e., stimuli presentation, customization of stimuli, or software synchronization of stimuli and EEG signal). These limitations made it challenging to design an experiment in which we could present auditory stimuli to patients and sync them with the EEG signal. To overcome this limitation, we externally generated auditory stimuli using a Raspberry Pi, presented them to patients via headphones, and built a

hardware trigger for synchronization. The trigger utilized the headset's plethysmograph photodiode that was originally intended for heart rate (HR) recording.

HR recordings are performed with a red- and infrared-light measuring photodiode (see diode location in Fig. 9). We connected a 3.3V LED to the Raspberry Pi (operated through the GPIO pins), attached it to the photodiode and covered the diode and LED with opaque tape (for placement, see Fig. 11 below). This way, the diode only records signal from the LED, which was set to blink in synchrony with the auditory stimuli (see full recording hardware in Figure 10 below). Later, the two information streams were synched, providing us with the stimuli locations in the EEG signal.

The LED was connected to the Raspberry Pi GPIOs with ~70cm of split-strand wires and a 330 Ohm resistor to prevent the LED from draining the Pi's battery or short-circuiting the LED (details Fig. 11).



Figure 9. Plethysmograph photodiode location on the Dreem headset. [Image](#) [Source](#). Annotation by author.



Figure 10. Full recording setup with LED attached to the Dreem headset.



Figure 11. [top] LED hardware with a 330 Ohm resistor. [bottom] Placement of the LED (Nichia NF2W757GT-F1-5080, 3 x 3 x 0.52 mm) on the plethysmograph diode.

Using this setup, auditory stimulation from the Pi can be synced with the LED blinks, which are visible on the plethysmograph signals. This allowed us to extract stimuli location indexes that are subsequently correlated with their corresponding EEG data stream locations by resampling from the plethysmograph's 50Hz sampling rate to the 250Hz EEG sampling rate. We found a large amount of regularly-distributed noise in the infrared-light signal, believed to be due to the diode being covered up fully (see Fig. 12, for example signals). A potential hypothesis for the noise in the infrared signal is that the device occasionally picks up on heat signals from the LED or the environment since heat is a form of infrared signal (Wang, 2011). Since such noise was absent in the red-light signal and stimuli locations appeared unimpacted by the noise in both signals, we chose to use the red-light signal to extract stimuli locations.

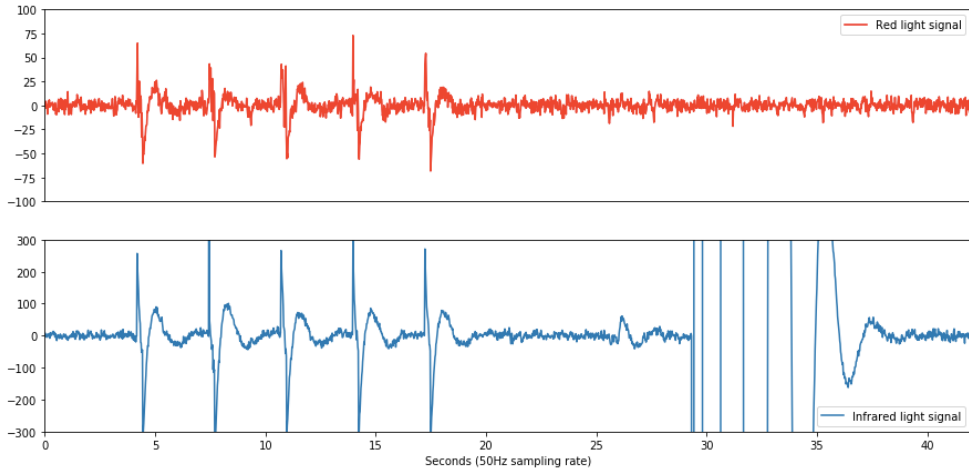


Figure 12. LED blinks in red-light [top] and infrared-light signal [bottom]. Note that the 5-blink stimuli trains are visible in both signals, but covering the photodiode generates regular noise signals in the infrared-light signal (bottom right). Because of this, only red-light signals were used to extract stimuli locations.

Auditory stimulation is spaced randomly throughout the day, with inter-stimuli-train times sampled from a Gamma distribution with a mean of 20 minutes (Fig. 13). Stimuli-trains consist of 5 consecutive 0.35s beeps at 600Hz, with an inter-stimulus interval of 3 seconds. Based on previous experience with how much high-quality data we can expect from a single recording, we anticipated ~55-100 clean stimuli-trains per 12-hour recording, giving us ~275-500 valid trials (for details about the simulation for these numbers, see Appendix 11.2).

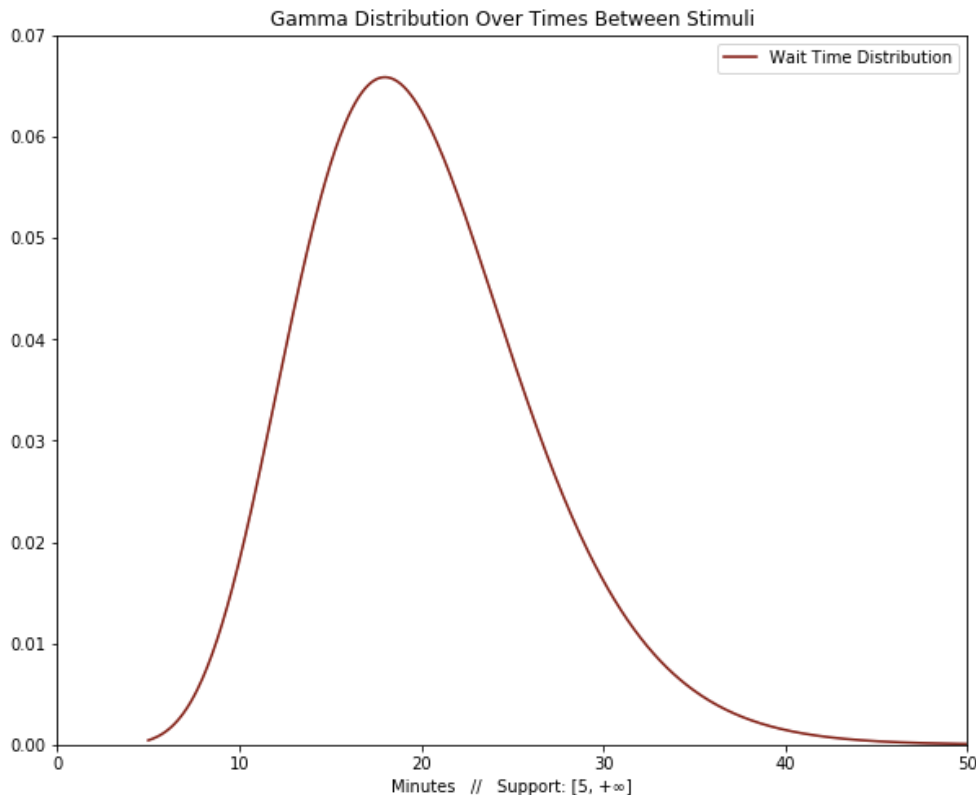


Figure 13. Gamma distribution over inter-stimuli-train wait times. Alpha-shape: 10, Beta-scale: 2. Mean wait time: 20 minutes. Support: $[5, +\infty]$.

To perform a recording session with the extended setup, researchers placed the Dreem headset with attached LED on the patient's head. A small screen and mouse were connected to the Pi, and the Pi was then be started up by connecting the fully charged battery pack. Running the [LED.py](#) file on the desktop (see Code 1), starts the auditory stimulation with a 1 minute setup period, a 5s trial blink, followed by the auditory stimulation (spaced as described above). The setup timer allows the researchers to disconnect the mouse and monitor and place the Pi in a convenient location for the patient. Alternatively, the [LED.py](#) file can be run before placing the headset on the patient's head, if connecting monitor and mouse right next to the patient causes difficulty. Ending the recordings works just like in the basic setup.

```

1. # GENERATING INTER-STIMULITRAIN TIMES
2. wait_time_distribution = sts.gamma(a=20, scale=2)
3. sample_times = wait_time_distribution.rvs(size=1000)
4.
5. sleep_times = []
6.
7. #appending ~12h (720 min) of wait times none smaller than 5min
8. #then converting them to seconds for time.sleep()
9. for t in sample_times:
10.     if t >= 5.0 and np.sum(sleep_times)/60 < 720:
11.         print(str(t), "minutes")
12.         t_in_sec = int(t * 60)
13.         sleep_times.append(t_in_sec)
14.
15. #PRE-RECORDING TRIALS
16. led = LED("GPIO14")           #set LED output
17. led.off()                   #clearing outputs to make sure LED is off
18.
19. time.sleep(60)              #setup period 1 minute
20. led.on()
21. print("on")
22. time.sleep(5)               #5sec trial run
23. led.off()
24. print("off")
25.
26.
27. def play_sound(duration, frequency): #defining sound function
28. """
29.     This function passes the stimulation parameters to the
30.     commandline "play" command.
31. """
32. os.system('play -n synth %s sin %s' %(duration, frequency))
33.
34. #EXPERIMENT
35. for t in sleep_times:
36.     time.sleep(t)             #inter-stimuli-train waittime
37.
38.     #with this setup, stimuli trains are ~17sec long between sleep
39.     #times
40.     for beep in range(5):    #beep 5 times
41.         led.on()
42.         play_sound(0.35, 600) #0.35sec, 600Hz beep
43.         led.off()
44.         time.sleep(3)        #wait 3 sec between beeps

```

Code 1. Generating Inter-stimuli-train wait-times from a gamma distribution, pre-recording trials, and the code for the stimulation during the experiment. Note that 0.35s is the shortest possible sound interval passable to `play_sound()` that can still be heard. The LED is on through the entire 0.35s. For full code, see Appendix 11.1.

4.3 Data Collection

EEG recording parameters	
Recording Device	Dreem 2
Sampling Frequency EEG	250 Hz
Sampling Frequency Pleth	50 Hz
Band-pass Filter	0.4Hz-18Hz
Notch Filters	50 Hz & 60Hz
Electrode Placement	Fp1, Fp2, F7, F8, O1, O2
Ground	Fp2
Channels	Fp1-O1, Fp1-O2, Fp1-F7, F8-F7 F7-O1, F8-O2, Fp1-F8, O1-O2

Table 1. Recording parameters of both experiments.
Information on filters comes from personal correspondence with Dreem researchers (D. Eden, November 6, 2019).

4.3.1 Experiment 1

Data for experiment 1 was collected by Konieczny, L. (2019, unpublished) from ALS patient LEK, in nine separate recording sessions over the course of approximately two months. At the point of writing, the patient has been in CLIS for roughly three years, with no reliable communication having been established since. In past recordings, the patient's apparent alpha peak was recorded at 3.8Hz, with decreased activity in the traditional alpha range of 8-13Hz. The signal topography appeared similar to a control group's frontal theta activity and parietal alpha range activity (Hohmann et al., 2018). Recording dates, as well as start times and recording duration, are described below (Table 2).

Session #	Date	Start	Length
01	22/10/18	13:33 + 2	10:31
02	14/11/18	14:58 + 1	10:01
03	19/11/18	14:00 + 1	09:05
04	27/11/18	09:04 + 1	10:19
05	29/11/18	14:59 + 1	10:07
06	05/12/18	18:04 + 1	11:54
07	07/12/18	15:01 + 1	10:00
08	10/12/18	18:05 + 1	05:43
09	13/12/18	16:20 + 1	09:42
---	---	---	---
Total time		---	87:22

Table 2. LEK patient data recordings summary.

Start times are presented in GMT with time shift; length is in hours.

4.3.2 Experiment 2 - Auditory Stimulation

As of the writing of this paper, the recordings for the second experiment are ongoing, and both stimulation and non-stimulation data are being recorded with a new patient by the University of Würzburg. Data analysis is ongoing as well.

4.4 Data Preprocessing

Several data-preprocessing steps were performed with the following aims, details on each are provided below.

- **Basic Preprocessing** - importing only relevant data from the Dreem, referencing the O1-O2 channel, generating copies of the data to support operations on it without overwriting the original data.
- **Visualization**
 - Raw data plots aid in investigating data quality and were particularly useful in debugging issues with syncing Pleth and EEG signals.

- Power spectra were used for general quality control to check if the expected alpha peak was visible in patient and non-patient recordings.
 - Spectrograms encode the same information as power spectra with the addition of a time axis; they are used as the basis for data annotation.
- **Annotation** - identifying and labeling clean data segments and artifacts such that they can be removed before an analysis is performed.
- **Short-Time Fourier Transformation (STFT)** - used to extract the features of interest, amplitude, and frequency, from the clean data.

4.4.1 Dreem Preprocessing

The Dreem h5 files come with seven channels of raw data and their corresponding "visualization" channels, which correspond to the raw data filtered using a band-pass filter between 0.4Hz and 18Hz and two notch filters at 50 and 60Hz. For the purpose of most analyses, the raw data channels without these provided filters were used, since features were extracted from frequencies outside the filters. The Dreem setup uses an internal synchronization procedure to ensure that the photodiode and EEG signal match up perfectly despite differences in sampling rate and minor potential drifts of the EEG signal (max 10s/8h period) (D. Eden, personal communication, November 6, 2019).

4.4.2 Basic Preprocessing

The data was retrieved from the dreemviewer.com internal Dreem data storage website in H5 format. It comes with 7 channels pre-calculated ('Fp1-O1', 'Fp1-O2', 'Fp1-F7', 'F8-F7', 'F7-O1', 'F8-O2', 'Fp1-F8'). 'O1-O2' was manually re-referenced for all recordings during data pre-processing (channel references follow the International 10-20 system; see Oostenveld & Praamstra, 2001).

During data import, large parts of the H5 file with secondary information relevant only to the original use of the Dreem, are discarded (i.e., sleep onset data, alarm clock timestamps, sleep stimulation information). Each file is tagged with meta-data (EEGPreprocess.data['info']), extracted from the file name, including patient name, recording number, and date.

For most plotting functions, the EEGProcessing class requires a data copy to be generated from the original H5 file and will not allow for it being overwritten or sliced directly. This is to prevent accidental overwriting of the

original data files. The *EEGProcessing.generate_copy()* function generates a copy of the original hierarchical dictionary, using the same key-value structure as the original data.

4.4.3 Visualizing the Data

The EEGProcessing Class supports three main data visualization functions: raw data plots, power spectra, and spectrograms. The raw data plots can be generated for any of the eight channels, as well as the pulse oximeter data. The *cut_raw()* function supports slicing specific recordings and channel selections and will automatically resize the pulse oximeter data to display the corresponding data sections.

Power spectra are generated using matplotlib's *psd()* (power spectral density) function, with the following hyperparameters: Fs=250 (sampling rate), NFFT=1024 (# of data points used per FFT block).

Spectrograms are generated with python's *scipy.signal.spectrogram()* function. It is passed the data with subtracted mean, based on data-chunks generated by the chosen 1-minute window-length, as well as the following hyperparameters: fs=250 (sampling frequency), noverlap=0 (no segment overlap). The color bars are adjusted from 0-15, providing the best visibility of the features.

4.4.4 Data Annotation

Visualization of the data as a raw data stream, power spectra and in particular spectrograms (1 minute time windows, no overlap) revealed that large portions of the data appeared useable, with artifacts being mainly limited to specific sections of each recording (i.e., the patient was moved during physiotherapy or happened to be in high electric noise area for a while).

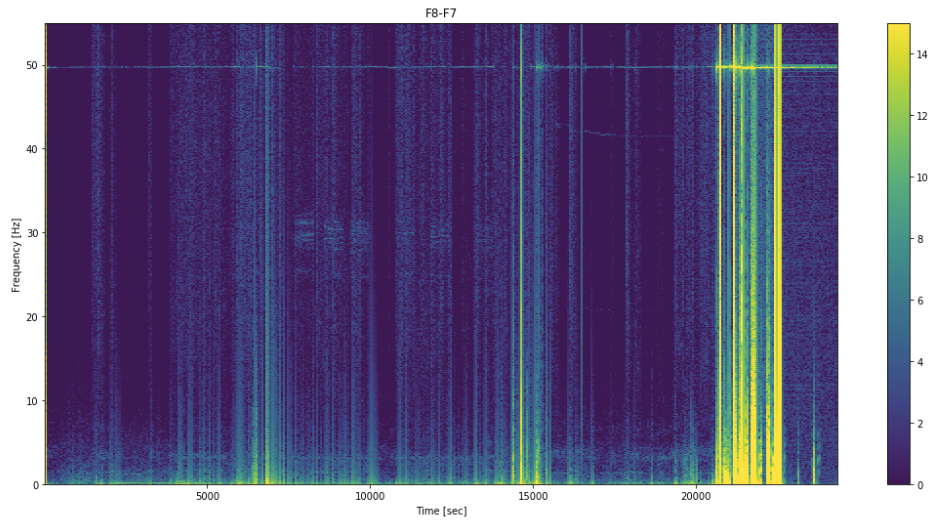


Figure 14. Example spectrogram plot of a single recording, single channel. On the right after the "20000" mark, a few minute long movement artifact can be seen. The 50Hz power outlet noise is also clearly visible.

Three additional artifact types emerged: "ripples" (of various kinds), "spotting" and a "drifting peak". The former two are believed to be amplifier saturation artifacts otherwise common in the 50Hz frequency range. The cause of drifting frequency peaks, as in the figure below (Fig. 15), is still unknown and can be explored during analysis.

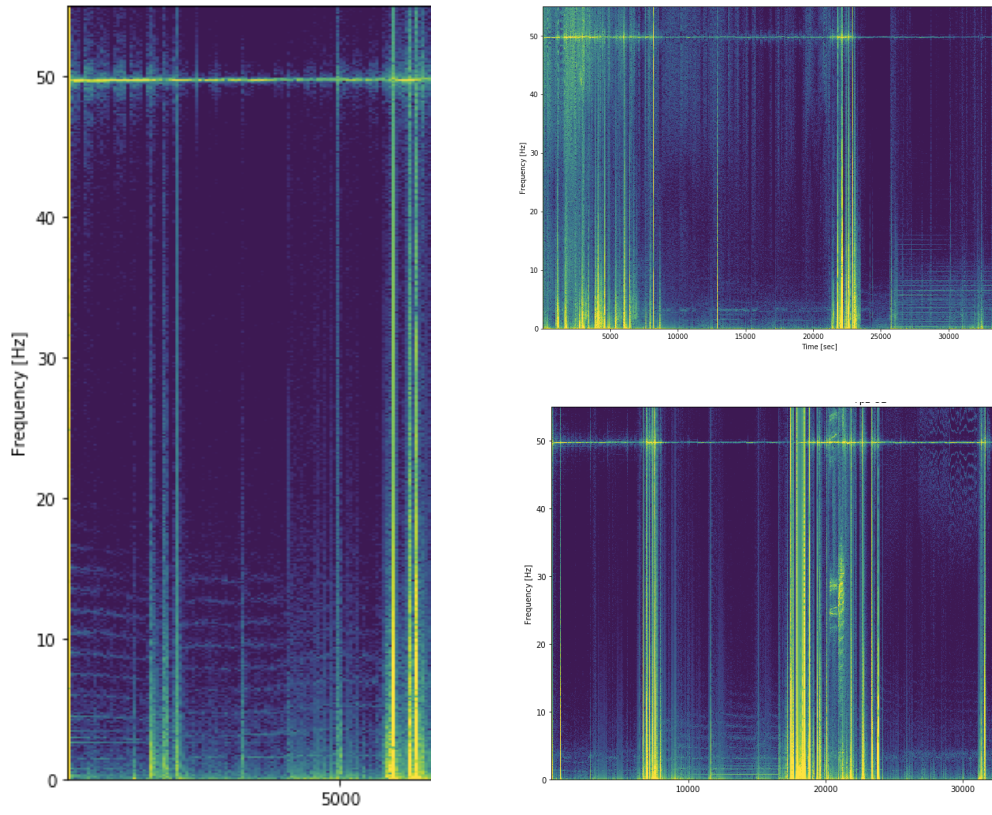


Figure 15. [left] "ripples" that occasionally appear in the 0-20Hz range. (rec8, O1-O2). [right, top] Extremely regular "ripples" at the bottom right. (rec4, F8-O2). [right, bottom] Another form of "ripples", in the top right corner of this recording. (rec6, Fp1-O2).

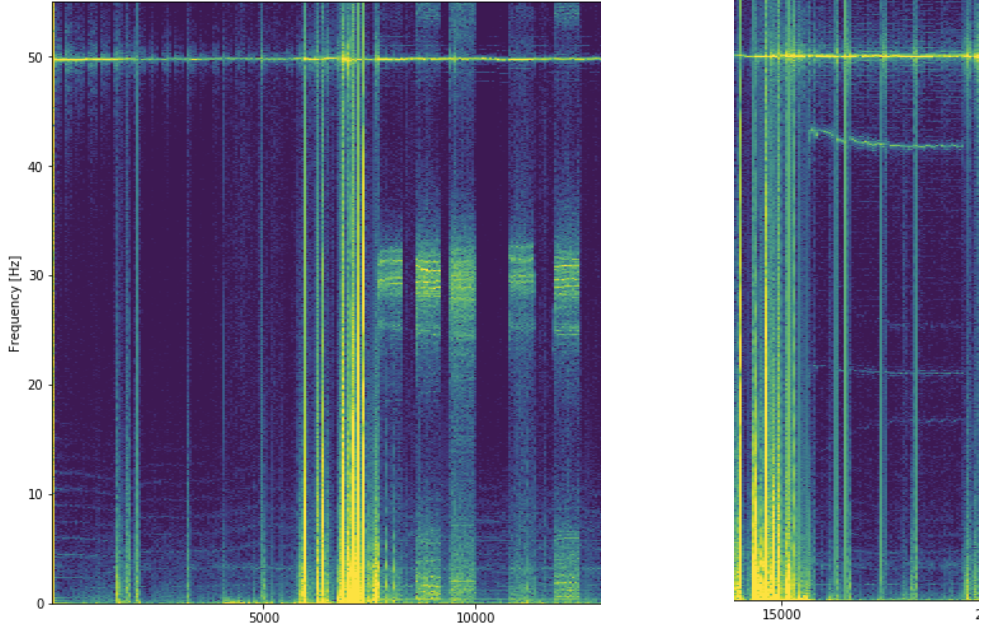


Figure 16. [left] "spotted" recording sections, common in the 10-50Hz range. (rec8, F8-O2). [right] example of "peak drift". This occurred at ~40Hz and is mirrored by lighter peaks in the 5-15Hz range. (rec8, F8-O2).

The data were manually labeled using a custom-built UI on the spectrogram plots. Data were separated into artifact-free, semi-artifact-free, rippled, spotted, peak-drift, post-recording (simply taking off the headset after the recording will leave an hour of non-cognitive recordings before the headset turns off) and noisy/other.

The Annotation UI allows for a section of the graph to be manually selected and the corresponding label to be typed in, which will then be saved as a list of labels for the selected indexes in the background (Fig. 17). This way, X and Y labels were generated for each recording.

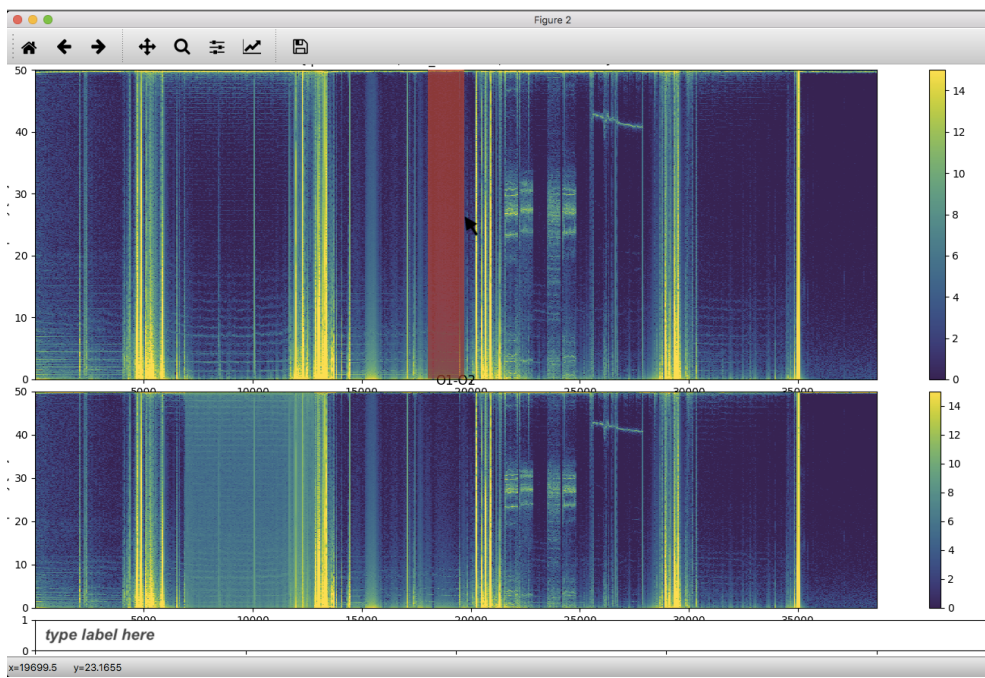
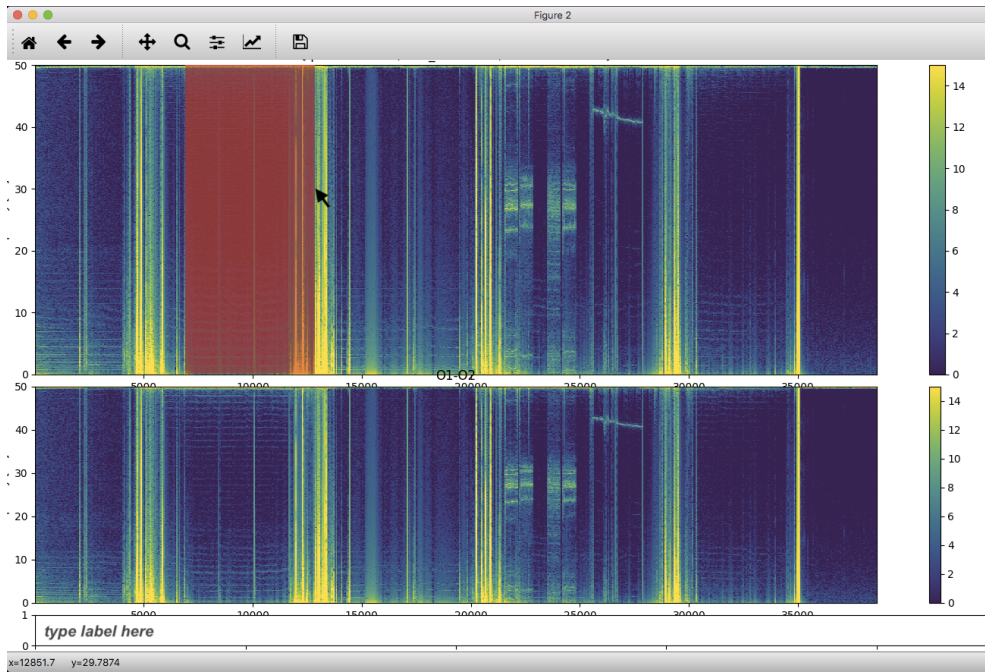


Figure 17. View of the data annotation UI. [top] using the cursor, sections of the data can be selected and will be highlighted in red. Then labels for them can be entered in the textbox. [bottom] After selection, a section will be highlighted on the graph to indicate that it has been processed. Then the user can select a new section.

X labels correspond to the dimensions of $(f, t, \# \text{ channels})$, where f and t are the frequency and time axis of the spectrogram plot. A recording's X label hence holds the information of each of its channels' spectrogram plot.

Y labels are of the dimensions $(t, \# \text{ channels})$. They correspond to a numerical label for each spectrogram 1-minute time window (0 if no annotation). Note that this means that labels are extrapolated for the raw data stream, and one "clean" label corresponds to a full 1-minute segment of the raw data.

4.4.5 Feature Extraction

Amplitude and Frequency peaks are extracted from the data using a short-time Fourier transformation (STFT), with time windows, input data, and overlap being the same as for the spectrogram function used for data annotation. An STFT is a way of extracting the information in a spectral plot (amplitude over frequency) of a long time-signal by dividing it into smaller segments to which to apply a Fourier transformation separately. Plotting this information over time would yield a spectrogram (hence the overlapping parameters with the spectrogram function).

The ranges for feature extraction were specified manually (2.5-4.5 Hz for "alpha" and 1-2.5Hz for "theta"), and the extraction function returns a single peak amplitude value for each minute of recording and the corresponding frequency at which the peak occurred. Applied to every recording and channel, the `stft feature extraction()` function returns a feature dictionary, where features are max amplitude and corresponding frequency of every recording and channel.

4.5 Data Analysis Methods Overview

To answer the guiding questions of this data analysis, the following analyses will be performed on the data:

- On the cleaned data, an STFT (short-time Fourier transform) will be used to extract the relevant frequency and amplitude information with 1-minute, non-overlapping windows.
- From this data, max amplitude (real part of the STFT results) in the down-shifted "alpha" (2.5-4.5Hz) and "theta" (1.0-2.5Hz) range will be extracted and their corresponding frequency retrieved for each of the 1-minute windows.

- These two frequency band peaks will be checked for auto-correlation patterns over time and correlation between each of them using scatter plots. If linear relationships emerge, correlation measures will be calculated.
- All recordings will be synced by their starting time to analyze patterns over the course of a day.
- Subsequently, frequency and amplitude of all frequency bands will be searched for interesting patterns of covariance over the course of the day using scatter plots and correlational measures where applicable.

5 Results

To remind the reader, the hypotheses I am investigating in this results section are:

- **H1:** There is a gradual reduction in mean "alpha" frequency over time.
- **H2:** Interesting patterns of co-variation between peak amplitude and frequency of different bands exist over time as well as throughout the course of a day.

The presented results first investigate the data quality that I was able to obtain from the Dreem headset and then, in order, presents investigative evidence for **H2**, investigating correlational patterns between peak amplitudes and their corresponding frequencies. First by looking at bi-variate correlational plots, then by subsequently investigating patterns of variation over the course of a day. Lastly, I present results for **H1**, showing the change of "alpha" throughout all recordings performed.

5.1 Data Quality of the Dreem Headset

A primary concern about recording data with the Dreem headset was data quality and if it would be sufficient for later analyses. Depending on channel and time of recording, the signal can be clear or noisy for long stretches of time (see Fig. 18 for comparison).

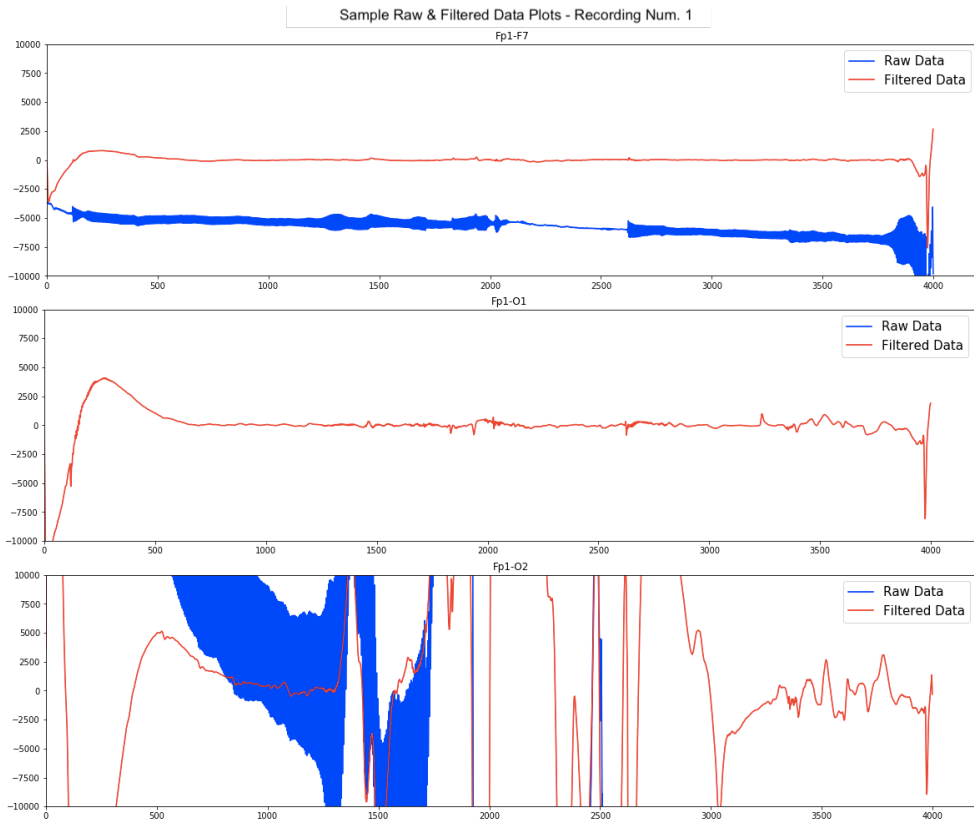


Figure 18. Sample raw data signals from 3 select channels over the same period (~16 minutes for recording).

These discrepancies become even more visible on the Spectrogram plots, where it becomes easy to visually distinguish between "clean" signal and movement and other artifacts (Fig. 19).

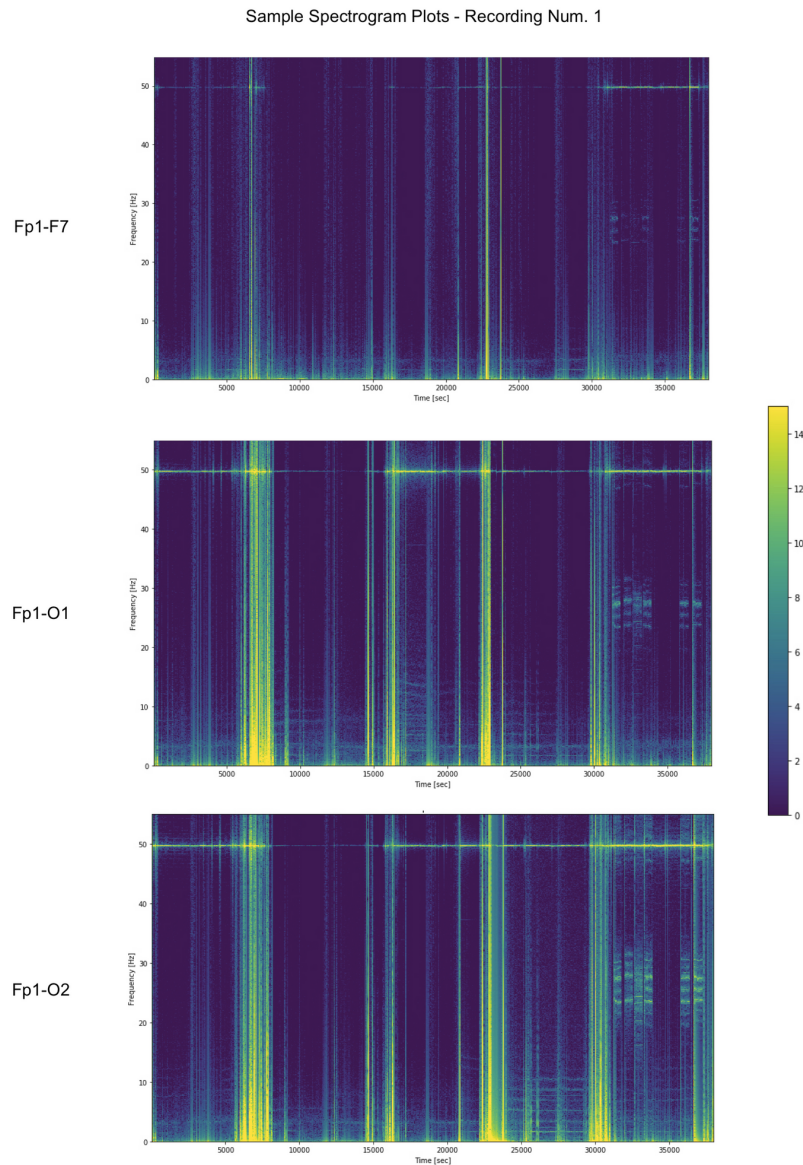


Figure 19. Sample Spectrogram plots, parameters as described in the above section. Sections of clean and noisy data are clearly visible. They sometimes, but not necessarily, align across channels.

Data cleaning allowed for clearer Power Spectra and improved analysis. For comparison, figure 20 (top and bottom) show a spectrogram prior to and after removing noisy data segments.

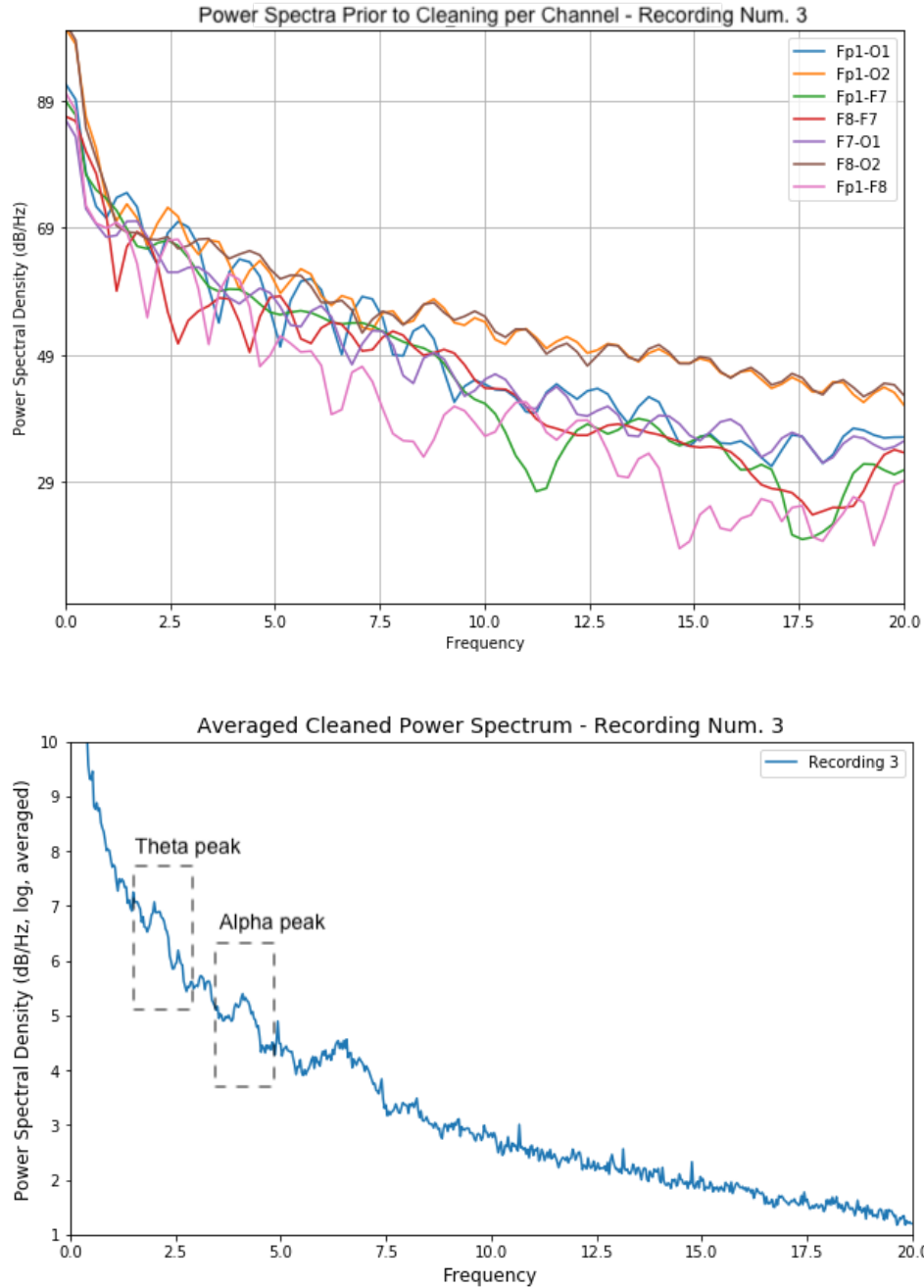


Figure 20. [top] Power Spectrum of recording before removing noisy data segments. [bottom] Averaged power spectrum with only clean data segments identified during annotation. Note how peaks in the Theta and Alpha range are now clearly visible.

5.2 Calculating Significance

In the following analysis, I plotted several types of correlation and time series to investigate the different hypotheses about the data.

P-values are calculated using a permutation test with 50.000 permutations for each p-value. Permutation tests are a commonly used, non-parametric way in bioinformatics to compute p-values when there is insufficient data for other methods. They are performed by comparing the test statistic value of the data to a distribution of test statistic values of the same data with labels randomly rearranged (Eddington & Onghena, 1980; Knijnenburg et al., 2009).

Each plot's p-value was corrected for generating multiple plots, using a Holm-Sidak multitest correction (Sidak, 1967).

For a combination of legibility and computational reasons¹, I chose to make a partial adjustment to plot p-values and also lower the p-value significance threshold α , by which to evaluate the provided p-values. I use the Holm-Sidak correction² on the alpha value together with the correction of the displayed p-values (details below). This should yield almost identical results to a Bonferroni correction (generally considered to be the strictest correction, comparative Bonferroni threshold: 0.0042), yielding only slightly higher power by making the assumption of test independence (Abdi, 2007). Using this correction, we can set the alpha threshold to be the following. Here, m is the number of comparisons performed.

$$\alpha_{\{per\ comparison\}}^* = 1 - (1 - \alpha)^{\frac{1}{m}} = 1 - (1 - 0.05)^{\frac{1}{12}} = 0.0043$$

In the following, I will only indicate results as significant if their p-values are below this threshold. Note that adjusting for p-values, alpha level, or partially adjusting both is equivalent under a Holm-Sidak correction. Correcting alpha by

¹ There's a tradeoff between tiny p-values (requiring a computationally expensive number of permutations) and ease of correction (collecting and correcting all p-values prior to plotting was infeasible in my code setup). Hence I combined both corrections here.

² Again, this was mostly a coding choice, since this function was readily available in the library I chose while being comparable to a Bonferroni correction.

a factor of 12 and p-values by a factor of 9 maintains the sample alpha-to-p-value ratio as adjusting the p-values by a factor of 108 (12x9) directly (IBM Support, 2018).

For each kind of plot, I have chosen to display a representative example, but in total, there are nine plots for each section (1 per recording, with the exception of the all-time frequency changes). I have performed twelve different hypothesis tests in my analysis (ten of which are shown here). Each section contains summary statistics of the plots that are provided in the Code Notebook Appendix (11.3). Summary statistics are shown as [mean \pm variance].

5.3 Describing Covariance

5.3.1 Within-band Covariance

The following figures show how peak frequency and the corresponding amplitude covary within each of the two frequency bands identified. For the alpha band (Fig. 21), most plots show small Pearson's r values $[-0.0004 \pm 0.011]$, and the corresponding p-values are insignificant $[0.501 \pm 0.101]$. For the theta band (Fig. 22), Pearson's r values are similarly small $[0.088 \pm 0.015]$ with insignificant p-values $[0.525 \pm 0.172]$. This suggests that the peak frequency of each individual band is not significantly correlated with its amplitude and would hence not make a useful measure of the patient's cognitive state for BCI communication.

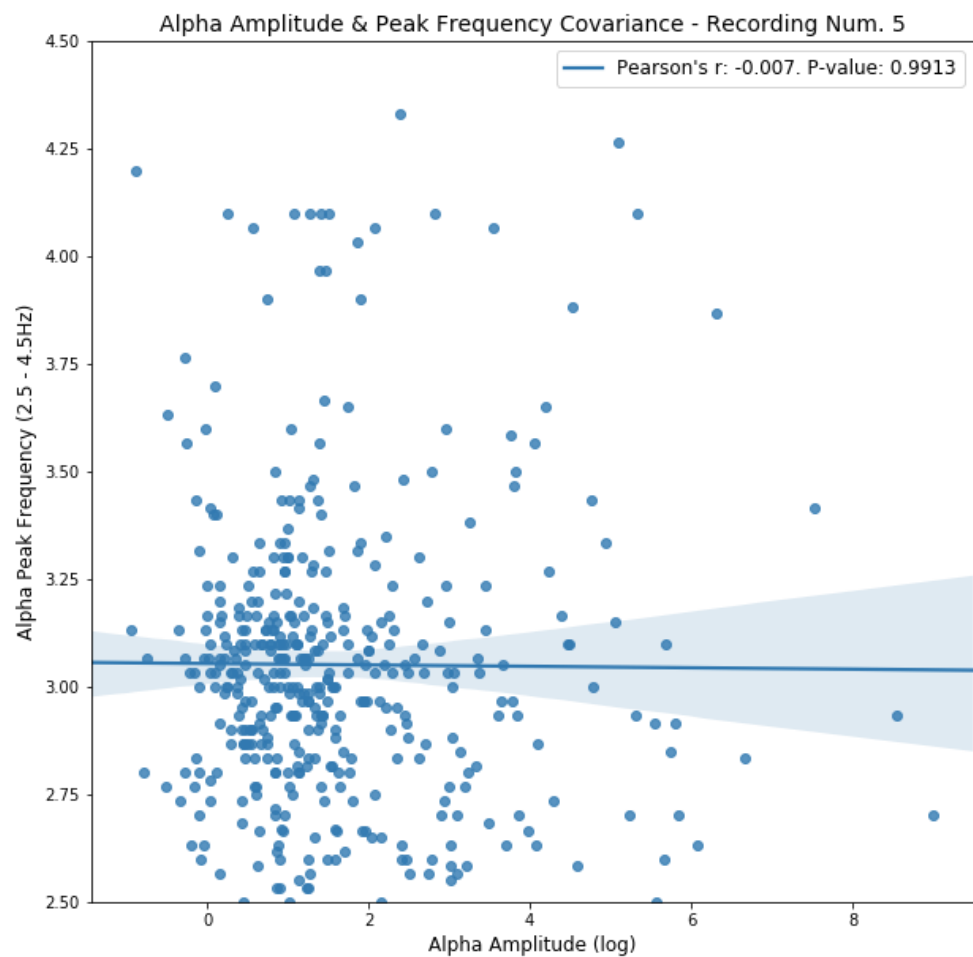


Figure 21. Sample alpha peak frequency for each time point (averaged over 60-second intervals), correlated with the corresponding alpha amplitude (log scale).

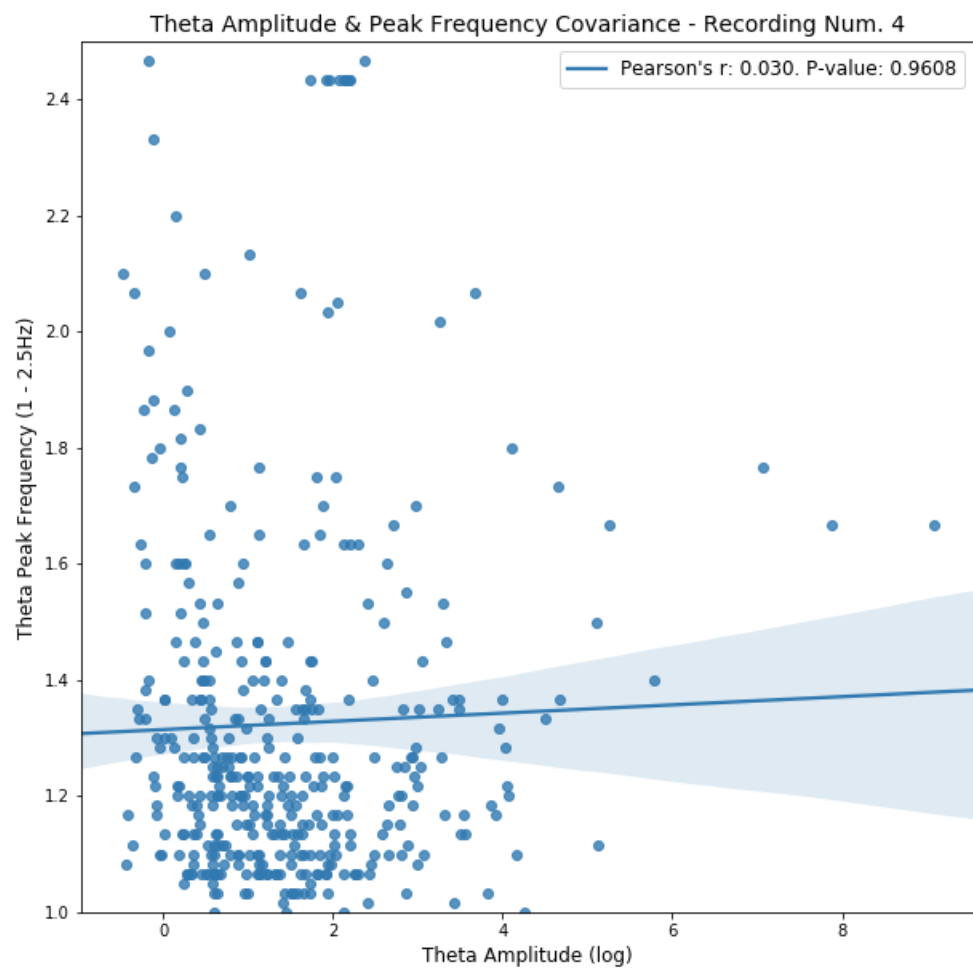


Figure 22. Sample theta peak frequency for each time point (averaged over 60-second intervals), correlated with the corresponding theta amplitude (log scale).

5.3.2 Frequency Covariance

Secondly, I compared the covariance of alpha and theta frequency peaks over the course of each recording (Fig. 23). The data showed a tendency for slight positive correlation [Pearson's $r: 0.162 \pm 0.018$], but without being significant [p -values: 0.213 ± 0.052]. This suggests that the two identified bands' peak frequencies do not significantly covary together. This finding corresponds to an intuitive understanding of the short-term behavior of the peak frequency as being rather invariant. Long-term shifts are analyzed in a later section.

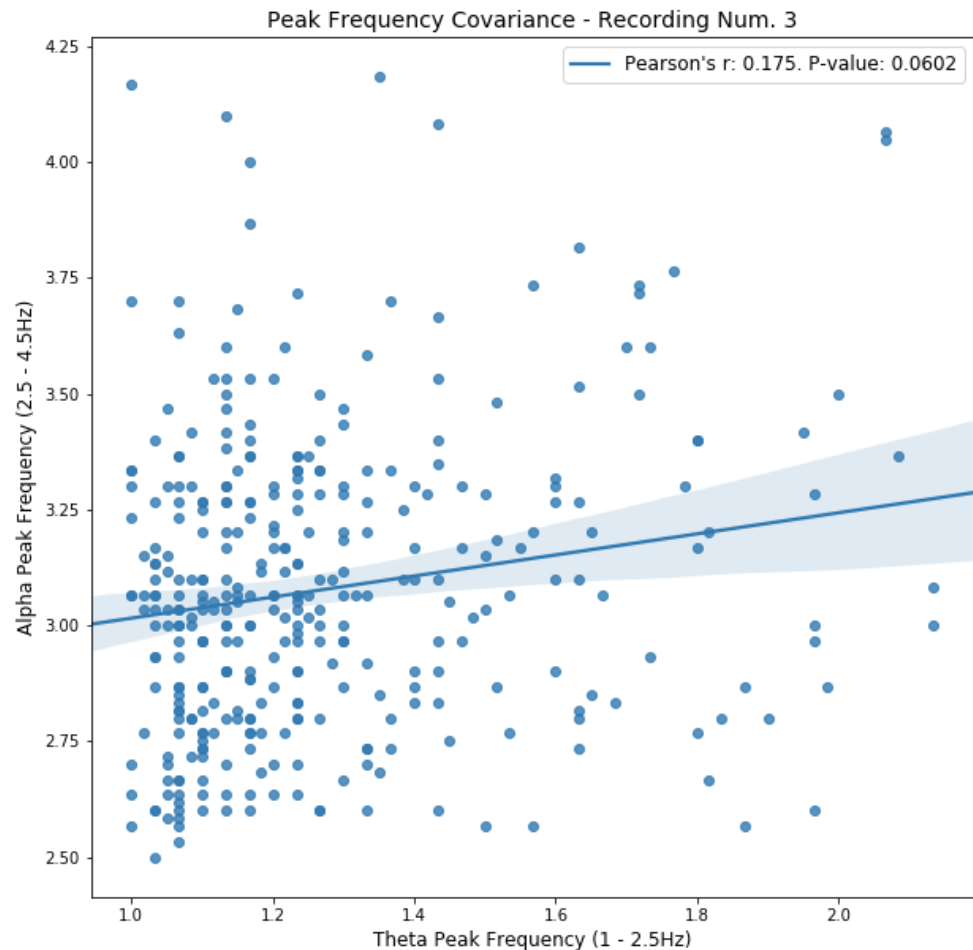


Figure 23. Sample covariance plot of alpha and theta peak frequencies.

5.3.3 Amplitude Covariance

Similarly, I correlated the amplitudes that corresponded to the peak alpha and theta values observed over time. They were strongly positively correlated [Pearson's r: 0.92 ± 0.0005] with significant p-values [0.0002 ± 0.0].

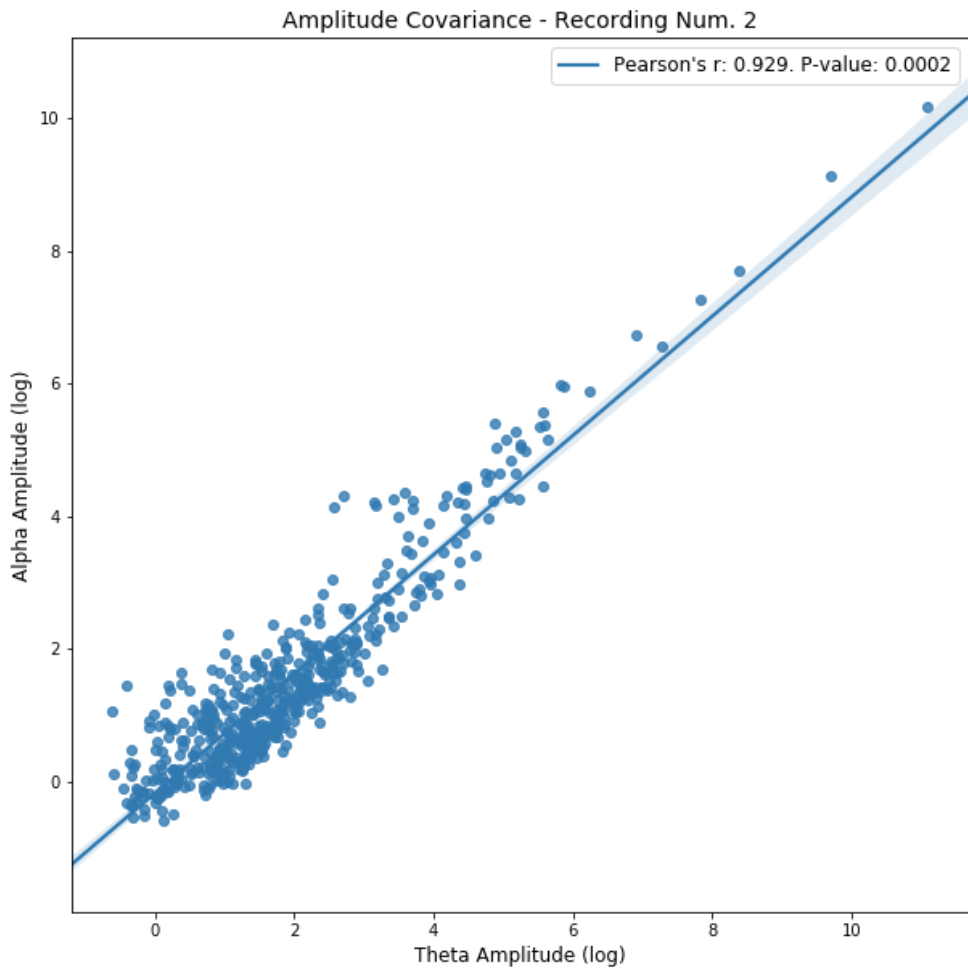


Figure 24. Sample amplitude covariance plot of alpha and theta log amplitude.

5.3.4 Amplitude - Outlier Corrected

Assuming that the strong covariance was potentially driven by outlier values (as Fig. 25 suggests), I performed a followup analysis, removing all outlier values, retaining only the 25th through 75th percentile of the data. This significantly reduces Pearson's r values [0.514 ± 0.015], but the positive correlation trend remains significant [p-values: 0.0002 ± 0.0].

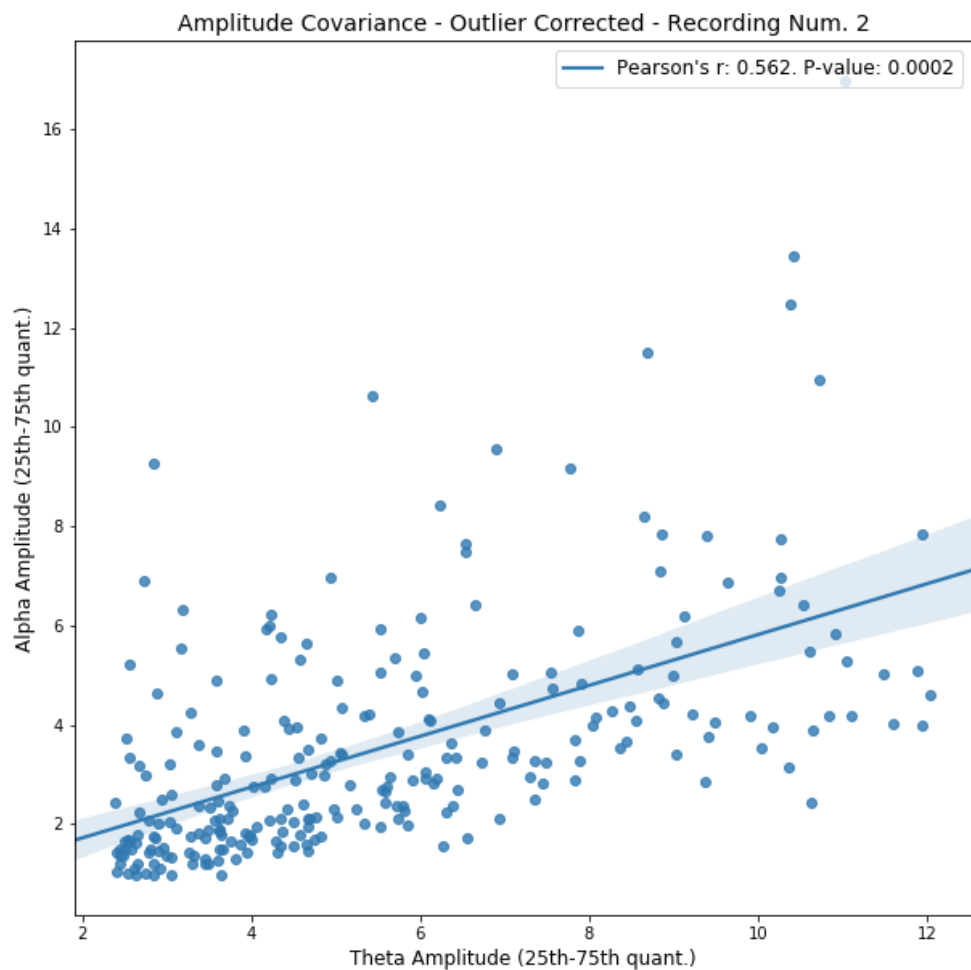


Figure 25. Sample amplitude covariance plot, with outlier correction performed (removing data points outside the 25th-75th quantile). Note that, excluding the outlier values, this plot can easily be visualized on a non-log plot.

5.3.5 Amplitude - Power & Outlier Corrected

In addition to it potentially being caused by outliers, a second hypothesis I tested was that variations in the total amplitude power may cause the trend (i.e., at time point t the overall amplitude was high due to device-specific variations, and hence the alpha and theta band are both high and covary strongly). In the following figure (Fig. 26), I corrected for variances in the total power of a given time point by scaling the data using the coefficients extracted from a linear regression model fitted to it. To allow comparison to the above plot (Fig. 25), I have also removed outliers in this plot. Pearson's r values [**0.514 ± 0.015**] and their corresponding p-values [**0.0002 ± 0.0**] suggest that the positive correlation persists when outliers are removed, and total power is corrected for. Note how close the values match the pre-power correction results. This suggests that total power has virtually no influence on the correlation, as is indicated in the code by receiving minimal slope adjustments and large shifts for both Theta and Alpha (hence the shift to negative numbers for the x- and y-axis here without a change in slope). In summary, this indicates that there is a noteworthy positive correlation between the amplitudes of the two frequency band peaks.

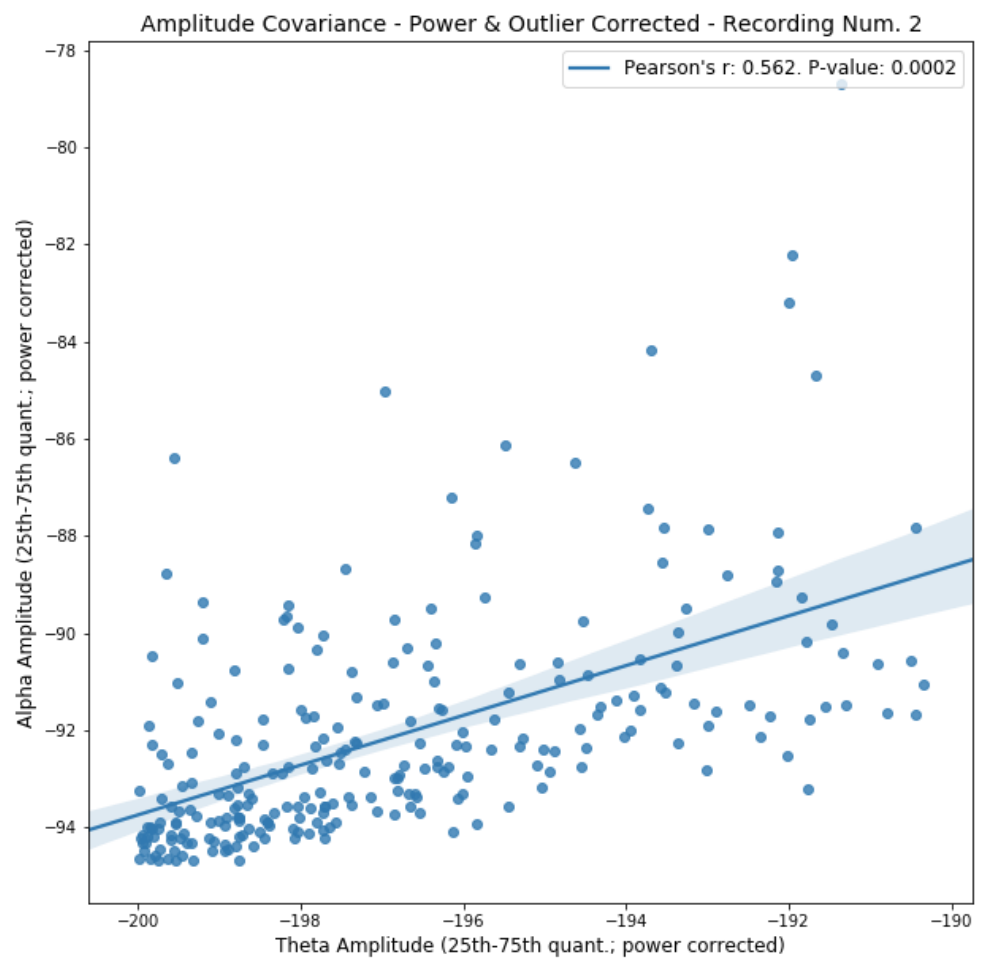


Figure 26. Sample amplitude covariance plot, corrected for total power of the recording, and with outlier correction performed (25th-75th quantile).

5.4 Amplitude and Frequency Over Time

5.4.1 Changes in Frequency

In addition to covariances, I was also interested in the patterns that alpha and theta peak frequencies display over the course of the day, with a particular interest in patterns that might emerge at specific times of the day, suggesting potential intervention times for BCI communication. For all time series plots, the sum over auto-correlation values squared was used as the test statistic.

$$y = \sum_t [AutoCorr.(x)^2]$$

Alpha peak frequency displayed no significant repetitive patterns across the day [p-values: 0.078 ± 0.122] and neither did the theta peak frequency [p-values: 0.030 ± 0.061]. As described above, the alpha significance threshold for these plots is *0.0043*.

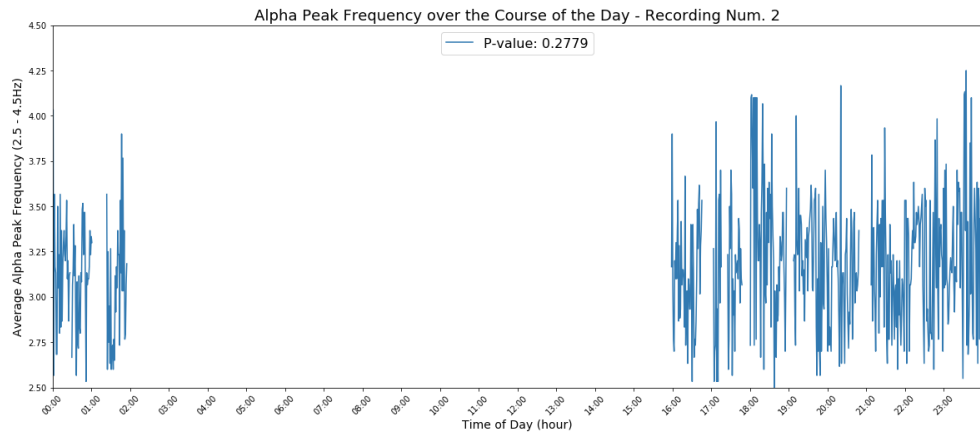


Figure 27. Alpha peak frequency variance across the course of a day. Data were aligned by start-time and wrapped around the 24-hour mark. In the above example, the recording started at 4 pm and lasted until approximately 2 am.

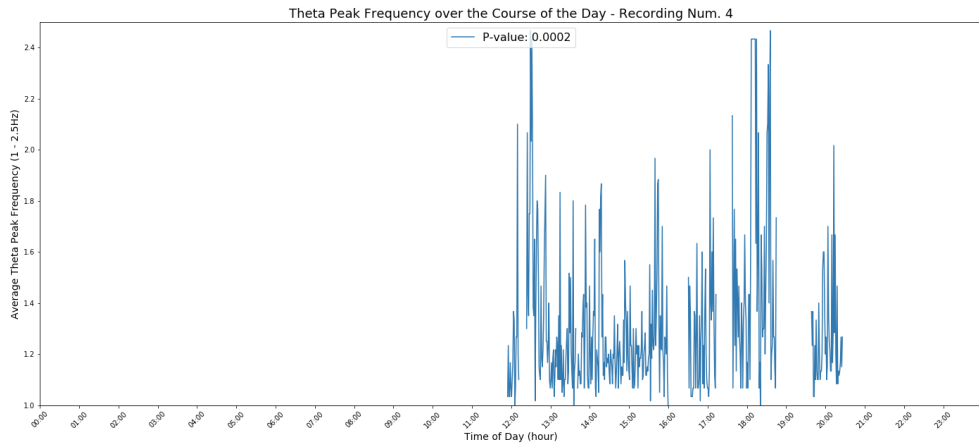


Figure 28. Theta peak frequency variance across the course of a day. Data were aligned by start-time, gaps in the recording correspond to noisy data segments. In the above example, the recording started at noon and lasted until approximately 8:30 pm, significant movement artifacts around 4 pm, 5:30 pm and 7 pm.

5.4.2 Changes in Alpha Over All Recordings

In line with Hohmann et al. (2018), figure 29 (top) shows the average alpha peak we observed across all recordings. I have also provided the trend-line for the Theta peak frequencies below (Fig. 29, bottom). The x-axis shows a total of 52 days of recordings, with data spread by the time that passed between them.

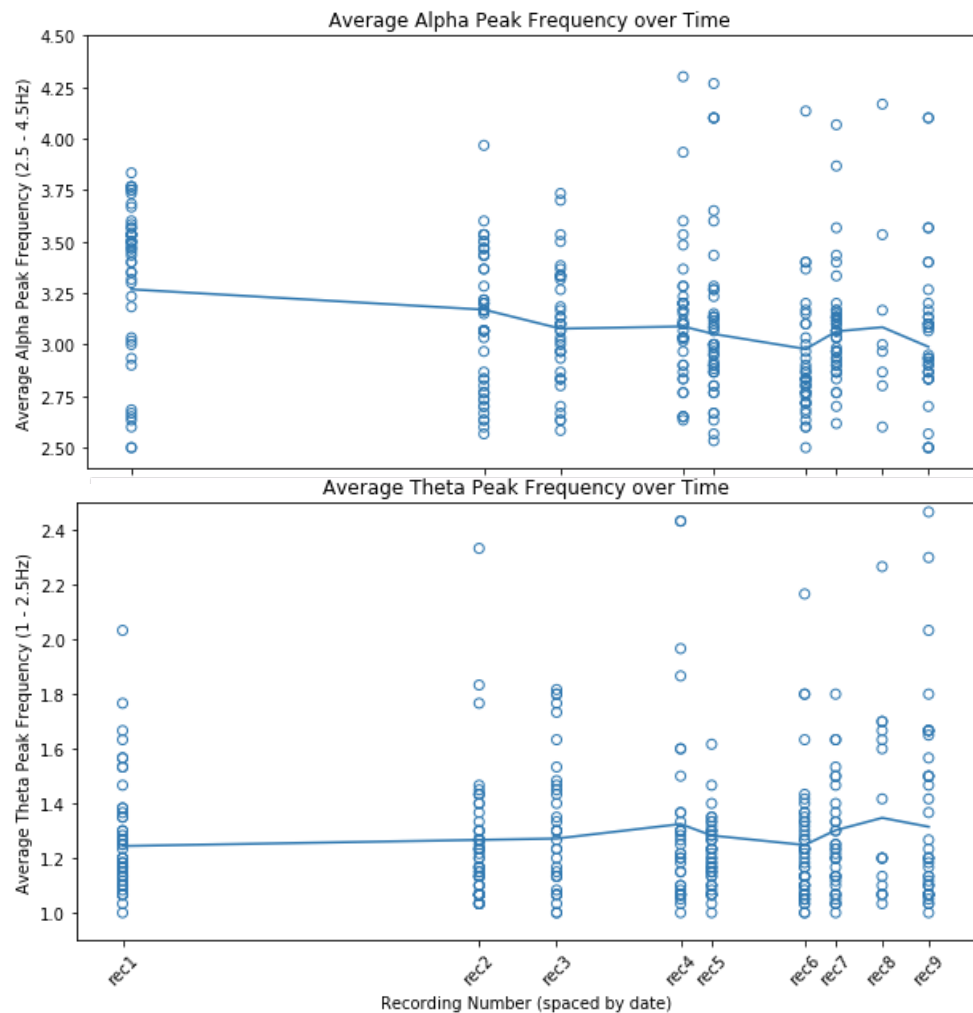


Figure 29. Average alpha [top] and theta [bottom] peak frequency over the course of all nine recordings. The x-axis is spaced by the time between recordings (52 days in total from recording 1 - 9). Points denote a randomly chosen 10% sample of the averaged alpha peak frequencies of that particular recording to show the distribution of the data.

6 Discussion and Conclusions

In conclusion, we have found that the data quality of the Dreem recordings, while of course not being comparable to an in-lab EEG system, is passable for simpler investigative needs. Given that recordings can be performed over hour-long periods at home, artifacts are more likely to occur (i.e., when the patient is moved during physical therapy or sleep). We chose to manually label clean data, which is labor-intensive, but relatively easy to do using spectrogram plots, as shown in Fig. 6. The plots show the clarity of the data, with a clearly visible 50Hz signal, little low-frequency noise and artifacts being limited to specific time periods. For this project, we chose to label each channel separately since the artifact-free periods did not fully align between channels. This is most likely the case because different electrodes had a better or worse connection to the skin at varying times. With more data available, we can envision a simpler labeling approach where spectrograms are averaged and all noisy segments discarded together. This would significantly reduce the amount of time needed for annotation at the cost of the amount of usable data.

We found no interesting connections between the peak frequency of a band and the corresponding amplitude, which means that when the alpha peak shifts to a higher frequency, this does not necessarily correspond to higher (or lower) activation at that time. Similarly, we did not find a clear indication for a correlation between the alpha and theta peak frequencies, or patterns of variance across the day, as we would have hoped to find. The follow-up experiment described in the methodology section (currently in the data collection stage) will provide evidence in favor of (or against) the hypothesis that the band we identified between 2.5-4.5Hz does, in fact, behave like an "alpha" band. The absence of correlation between the two, observed in our current data set, could be reinterpreted based on those results.

The most significant correlation observed was that of the positive amplitude correlation between alpha and theta. We adjusted those values accounting for the potential of the effect being outlier driven or due to overall changes in total power observed (potentially hardware related). The correlation, however, remained positive and significant with Pearson's r values of **0.514 ± 0.015** across all nine recordings performed. This finding directly contradicts past research, suggesting that alpha and theta are anti-correlated (see Sauseng et al., 2005; Klimesch, 1999; for examples). Potential hypotheses that could explain this finding are that the activation we have labeled "theta" in this experiment is, in fact, not a traditional theta activation and instead behaves like delta activation,

syncing, rather than desyncing with our “alpha” signal. Alternatively, it is possible that the observed alpha does not share properties with a traditional alpha. The follow-up experiment described is aimed at providing further evidence to support or refute this hypothesis in particular. Lastly, it is worth mentioning that the observed effect, while statistically significant, could be limited to the individual subject we observed in this study, which is likely the case, given the heterogeneity of alpha activation (Ringholz, 2005; Klimesch, 1999).

While the behavior of activation observed does not align with our initial hypotheses, it is noteworthy that for both alpha and theta, the data distribution is right/upward skewed, leaving few peaks to be picked up in the 2- 2.5Hz range (Fig. 29, bottom), which suggests that the two frequency bands we observed are, in fact, separate phenomena.

Finally, we would like to observe that there appears to be a general downward trend of the average alpha peak frequency (Fig. 29, top) that would support the hypothesis that there is a slow shift of the alpha peak to lower frequency ranges (Hohmann et al., 2018). The spread of the data, however, is far, and without access to past or future data, the period of time we observed with our nine recordings is too short (only 52 days) to observe a significant decrease in alpha. We would like to encourage future researchers to calculate average alpha peaks and observe if there are significant decreases in their patients more extended time periods.

We hope that the future data collection during the described follow-up experiment that is currently in progress can shed light on the patterns observed in the current data set and strengthen or refute some of the hypotheses we present in this analysis.

7 Glossary

ALS - Amyotrophic Lateral Sclerosis, is a rare (prevalence: 5.2 per 100.000) and fatal neurodegenerative disease characterized by motor neuron degeneration in the spinal cord, brainstem, corticospinal tract, and the primary motor cortex. The neuron degeneration leads to progressive muscular paralysis (Wijesekera & Leigh, 2009).

BCI - Brain-computer interfaces are devices that enable a communication pathway between the brain and a technical device. In most current use-cases they serve to bring rudimentary communication abilities to patients with physical or other disabilities (e.g., to control a prosthetic in stroke patients, express desires in locked-in patients, etc.)

Electrocorticography - Recording of electrical signal from electrodes placed directly on the surface of the brain. This is a common form of invasive BCI recording.

Electroencephalography - Recording of electrical signal from electrodes based on the scalp. This is a common form of non-invasive BCI recording.

Electromyography - Recording of electrical activity through electrodes placed on different muscles. In the presented work, this applies specifically to facial muscles and the external anal sphincter.

Electrooculography - Recording of electrical activity from a patient's eye by placing electrodes near the eye. This can be used to track eye movement.

ERP - Signal based on a cortical reaction to an external event that generates an Event-related potential. This potential can be used to drive BCI communication and is a commonly used method in the BCI field, as it requires little training. An example of ERP-based BCI would be a P300-speller.

GPIOs - general-purpose input/output pins along the top edge of the board of a Raspberry Pi (Raspberry Pi Documentation, 2019). They serve to generate voltage output (i.e., to power external devices such as an LED) and receive input (i.e., a grounded electrode receiving the electricity that flows through the LED from an output pin).

LIS & CLIS - Locked-in state and completely locked-in state are the two states often distinguished in ALS disease progression. A locked-in state is

characterized by complete paralysis with remaining voluntary eye movement or minimal facial muscle control (Kübler & Birbaumer, 2008). Communication is limited to eye movements or blinking. The completely locked-in state describes a later stage of the disease progression in which voluntary eye movement control ceases entirely.

Slow Cortical Potentials - Signal based on electrical activity in the brain at usually less than 1Hz (Neurofeedback Alliance, n.d.). With training, patients can learn to manipulate these potentials to generate BCI signals.

STFT - Short-time Fourier Transformation is a transformation performed on wave-shaped data to determine the decomposition of a wave into its constituent frequencies and how they change over time. The STFT divides a longer time signal into shorter segments of equal length and then computes the Fourier transform separately on each shorter segment. The changing spectra over time can be visualized as a spectrogram plot (Wikipedia, 2020).

Plethysmograph Photodiode - A photodiode is a light-sensitive semiconductor diode that generates an electrical signal when exposed to light. The diode on the Dreem is used as a plethysmograph (heart rate sensor) by emitting light that penetrates the skin and is reflected off blood vessels in a pattern that can be used to determine a patient's heart rate.

8 Bibliography

- Abdi, H. (2007). *The Bonferroni and Šidák Corrections for Multiple Comparisons*. Retrieved from <http://www.utd.edu/>
- Başar, E., Schürmann, M., Başar-Eroglu, C., & Karakaş, S. (1997). Alpha oscillations in brain functioning: An integrative theory. *International Journal of Psychophysiology*, 26(1–3), 5–29. [https://doi.org/10.1016/S0167-8760\(97\)00753-8](https://doi.org/10.1016/S0167-8760(97)00753-8)
- Başar, E., Başar-Eroglu, C., Karakaş, S., & Schürmann, M. (2001). Gamma, alpha, delta, and theta oscillations govern cognitive processes. *International Journal of Psychophysiology*, 39(2–3), 241–248. [https://doi.org/10.1016/S0167-8760\(00\)00145-8](https://doi.org/10.1016/S0167-8760(00)00145-8)
- Brownell, B., Oppenheimer, D. R., & Hughes, J. T. (1970). The central nervous system in motor neurone disease. *Journal of Neurology, Neurosurgery, and Psychiatry*, 33(3), 338–357. <https://doi.org/10.1136/jnnp.33.3.338>
- Cozzolino, M., Ferri, A., & Teresa Carri, M. (2008). Amyotrophic Lateral Sclerosis: From Current Developments in the Laboratory to Clinical Implications. *Antioxidants & Redox Signaling*, 10(3), 405–444. <https://doi.org/10.1089/ars.2007.1760>
- Edgington, E., & Onghena, P. (2007). Randomization Tests. In *CRC Press* (Fourth Edi). CRC Press.
- Finnigan, S., & Robertson, I. H. (2011). Resting EEG theta power correlates with cognitive performance in healthy older adults. *Psychophysiology*, 48(8), 1083–1087. <https://doi.org/10.1111/j.1469-8986.2010.01173.x>
- Fomina, T., Lohmann, G., Erb, M., Ethofer, T., Schölkopf, B., & Grosse-Wentrup, M. (2016). Self-regulation of brain rhythms in the precuneus: a novel BCI paradigm for patients with ALS. *Journal of Neural Engineering*, 13(6), 066021. <https://doi.org/10.1088/1741-2560/13/6/066021>
- Frank, B., Haas, J., Heinze, H. J., Stark, E., & Münte, T. F. (1997). Relation of neuropsychological and magnetic resonance findings in amyotrophic lateral sclerosis: Evidence for subgroups. *Clinical Neurology and Neurosurgery*, 99(2), 79–86. [https://doi.org/10.1016/S0303-8467\(96\)00598-7](https://doi.org/10.1016/S0303-8467(96)00598-7)
- Givens, B., & Olton, D. S. (1995). Bidirectional Modulation of Scopolamine-Induced Working Memory Impairments by Muscarinic Activation of the Medial Septal Area. *Neurobiology of Learning and Memory*, 63(3), 269–276. <https://doi.org/10.1006/nlme.1995.1031>
- GPIO. (2019). Retrieved from Raspberry Pi Documentation website: <https://github.com/raspberrypi/documentation/blob/master/usage/gpio/README.md>
- Grosse-Wentrup, M. (2019). The Elusive Goal of BCI-based Communication with CLIS-ALS Patients. *7th International Winter Conference on Brain-Computer Interface, BCI 2019*. <https://doi.org/10.1109/IWW-BCI.2019.8737310>
- Hackl, M. (2018). Disease detection in ALS patients using DTI and conventional MRI. [Course Assignment].
- Hohmann, M. R., Fomina, T., Jayaram, V., Emde, T., Just, J., Synofzik, M., ... Grosse-Wentrup, M. (2018). Case series: Slowing alpha rhythm in late-stage ALS patients. *Clinical Neurophysiology*, 129(2), 406–408. <https://doi.org/10.1016/j.clinph.2017.11.013>

- Hohmann, M. R., Hackl, M., Wirth, B., Zaman, T., Enficiaud, R., Grosse-Wentrup, M., & Schölkopf, B. (2019). MYND: A platform for large-scale neuroscientific studies. *Extended Abstracts of the 2019 CHI Conference on Human Factors in Computing Systems - CHI EA '19*, 1–6. <https://doi.org/10.1145/3290607.3313002>
- Kiloh, A., McComas, J., & Osselton, J. W. (1972). Clinical Electroencephalography. In *British Journal of Psychiatry* (3rd Editio). <https://doi.org/10.1192/bjp.122.4.486>
- Kim, D. W., Lee, J. C., Park, Y. M., Kim, I. Y., & Im, C. H. (2012, March). Auditory brain-computer interfaces (BCIs) and their practical applications. *Biomedical Engineering Letters*, Vol. 2, pp. 13–17. <https://doi.org/10.1007/s13534-012-0051-1>
- Klimesch, W. (1999). EEG alpha and theta oscillations reflect cognitive and memory performance: a review and analysis. *Brain Research. Brain Research Reviews*, 29(2–3), 169–195. Retrieved from <http://www.ncbi.nlm.nih.gov/pubmed/10209231>
- Knijnenburg, T. A., Wessels, L. F. A., Reinders, M. J. T., & Shmulevich, I. (2009, June 15). Fewer permutations, more accurate P-values. Retrieved March 12, 2020, from Bioinformatics website: <https://www.ncbi.nlm.nih.gov/pmc/articles/PMC2687965/>
- Kübler, A., & Birbaumer, N. (2008). Brain–computer interfaces and communication in paraparesis: Extinction of goal directed thinking in completely paralysed patients? *Clinical Neurophysiology*, 119(11), 2658–2666. <https://doi.org/10.1016/j.clinph.2008.06.019>
- Laureys, S., Gosseries, O., & Tononi, G. (2009). *The Neurology of Consciousness: Cognitive Neuroscience and Neuropathology* (2nd Editio).
- Marchetti, M., & Priftis, K. (2015). Brain-computer interfaces in amyotrophic lateral sclerosis: A metaanalysis. *Clinical Neurophysiology*, 126(6), 1255–1263. <https://doi.org/10.1016/j.clinph.2014.09.017>
- Massman, P. J., Sims, J., Cooke, N., Haverkamp, L. J., Appel, V., & Appel, S. H. (1996). Prevalence and correlates of neuropsychological deficits in amyotrophic lateral sclerosis. *Journal of Neurology Neurosurgery and Psychiatry*, 61(5), 450–455. <https://doi.org/10.1136/jnnp.61.5.450>
- Murguijalday, A. R., Hill, J., Bensch, M., Martens, S., Halder, S., Nijboer, F., ... Gharabaghi, A. (2011). Transition from the locked in to the completely locked-in state: A physiological analysis. *Clinical Neurophysiology*, 122(5), 925–933. <https://doi.org/10.1016/j.clinph.2010.08.019>
- Neumann, N., & Kotchoubey, B. (2004). Assessment of cognitive functions in severely paralysed and severely brain-damaged patients: Neuropsychological and electrophysiological methods. *Brain Research Protocols*, 14(1), 25–36. <https://doi.org/10.1016/j.brainresprot.2004.09.001>
- Niedermeyer, E., & Silva, F. da. (2005). *Electroencephalography: basic principles, clinical applications, and related fields*. Retrieved from <https://books.google.com/books?hl=en&lr=&id=tndqYGPHQdEC&oi=fnd&pg=PR11&dq=Electroencephalography:+basic+principles,+clinical+applications,+and+related+fields,&ots=GODi594akw&sig=uz'od-yQVanohDNIXjQjH5JGQkM>
- Nijboer, F., Sellers, E. W., Mellinger, J., Jordan, M. A., Matuz, T., Furdea, A., ... Kübler, A. (2008). A P300-based brain-computer interface for people with amyotrophic lateral sclerosis. *Clinical Neurophysiology*, 119(8), 1909–1916. <https://doi.org/10.1016/j.clinph.2008.03.034>
- Nijboer, F., Furdea, A., Gunst, I., Mellinger, J., McFarland, D. J., Birbaumer, N., & Kübler, A. (2008). An auditory brain–computer interface (BCI). *Journal of Neuroscience Methods*, 167(1), 43–50. <https://doi.org/10.1016/j.jneumeth.2007.02.009>

- Oostenveld, R., & Praamstra, P. (2001). The five percent electrode system for high-resolution EEG and ERP measurements. *Clinical Neurophysiology*, 112(4), 713–719. [https://doi.org/10.1016/S1388-2457\(00\)00527-7](https://doi.org/10.1016/S1388-2457(00)00527-7)
- Ringholz, G. M., Appel, S. H., Bradshaw, M., Cooke, N. A., Mosnik, D. M., & Schulz, P. E. (2005). Prevalence and patterns of cognitive impairment in sporadic ALS. *Neurology*, 65(4), 586–590. <https://doi.org/10.1212/01.wnl.0000172911.39167.b6>
- Rocha, J. A., Reis, C., Simões, F., Fonseca, J., & Mendes Ribeiro, J. (2005). Diagnostic investigation and multidisciplinary management in motor neuron disease. *Journal of Neurology*, 252(12), 1435–1447. <https://doi.org/10.1007/s00415-005-0007-9>
- Sauseng, P., Klimesch, W., Schabus, M., & Doppelmayr, M. (2005). Fronto-parietal EEG coherence in theta and upper alpha reflect central executive functions of working memory. *International Journal of Psychophysiology*, 57(2), 97–103. <https://doi.org/10.1016/j.ijpsycho.2005.03.018>
- Shaw, P. J. (2005). Molecular and cellular pathways of neurodegeneration in motor neurone disease. *Journal of Neurology, Neurosurgery & Psychiatry*, 76(8), 1046–1057. <https://doi.org/10.1136/jnnp.2004.048652>
- Short-time Fourier transform. (2020). Retrieved February 21, 2020, from Wikipedia the Free Encyclopedia website: https://en.wikipedia.org/wiki/Short-time_Fourier_transform
- Šidák, Z. (1967). Rectangular Confidence Regions for the Means of Multivariate Normal Distributions. *Journal of the American Statistical Association*, 62(318), 626–633. <https://doi.org/10.1080/01621459.1967.10482935>
- Signorino, M., Pucci, E., Belardinelli, N., Nolfe, G., & Angeleri, F. (1995). EEG spectral analysis in vascular and Alzheimer dementia. *Electroencephalography and Clinical Neurophysiology*, 94(5), 313–325. [https://doi.org/10.1016/0013-4694\(94\)00290-2](https://doi.org/10.1016/0013-4694(94)00290-2)
- Slow Cortical Potential Training. (n.d.). Retrieved February 21, 2020, from Neurofeedback Alliance website: <http://neurofeedbackalliance.org/slow-cortical-potential-training/>
- The calculation of Bonferroni-adjusted p-values. (2018). Retrieved March 12, 2020, from IBM Support website: <https://www.ibm.com/support/pages/calculation-bonferroni-adjusted-p-values>
- Van Dijk, H., Nieuwenhuis, I. L. C., & Jensen, O. (2010). Left temporal alpha band activity increases during working memory retention of pitches. *European Journal of Neuroscience*, 31(9), 1701–1707. <https://doi.org/10.1111/j.1460-9568.2010.07227.x>
- Vlahou, E. L., Thurm, F., Kolassa, I. T., & Schlee, W. (2014). Resting-state slow wave power, healthy aging and cognitive performance. *Scientific Reports*, 4(1), 1–6. <https://doi.org/10.1038/srep05101>
- Wang, W.-C. (2011). *Optical Detectors*. Retrieved from <https://depts.washington.edu/mictech/optics/me557/detector.pdf>
- Wang, Y., Gao, X., Hong, B., & Gao, S. (2009). *Practical Designs of Brain–Computer Interfaces Based on the Modulation of EEG Rhythms*. https://doi.org/10.1007/978-3-642-02091-9_8
- Weisz, N., Hartmann, T., Müller, N., Lorenz, I., & Obleser, J. (2011). Alpha rhythms in audition: Cognitive and clinical perspectives. *Frontiers in Psychology*, 2(APR). <https://doi.org/10.3389/fpsyg.2011.00073>
- Wijesekera, L. C., & Leigh, P. N. (2009). Amyotrophic lateral sclerosis. *Orphanet Journal of Rare Diseases*, 4(1), 3. <https://doi.org/10.1186/1750-1172-4-3>

Wilkinson, R. T., & Allison, S. (1989). Age and simple reaction time: Decade differences for 5,325 subjects. *Journals of Gerontology*, 44(2).
<https://doi.org/10.1093/geronj/44.2.p29>

9 Appendix

9.1 Code for Inter-Stimuli Wait-times

```
1. import time
2. import numpy as np
3. from gpiozero import LED
4. import scipy.stats as sts
5. import os
6.
7. ## MAIN FUNCTION CALL
8. print("SETTING UP EXPERIMENT")
9.
10. #generating wait times from a gamma distribution (like poisson,
11. #but continuous so I can sample more precise minute intervals)
12. #setting alpha to be 10 minutes and beta = 2 will give us a distribution with
13. #larger spread than simply (20,1), while keeping the mean at 20 minutes
14. #rejection sampling to get only samples larger than 5min
15. #check homepage.divms.uiowa.edu/~mbognar/applets/gamma.html for a visualization
16. # tool of this distribution
17.
18. wait_time_dist = sts.gamma(a=20, scale=2)
19. sample_times = wait_time_dist.rvs(size=1000)
20.
21. wait_times = []
22.
23. #appending ~12h (720 min) of wait times none smaller than 5min
24. #then converting them to seconds for time.sleep()
25. for t in sample_times:
26.     if t >= 5.0 and np.sum(wait_times)/60 < 720:
27.         print(str(t), "minutes")
28.         t_in_sec = int(t * 60)
29.         wait_times.append(t_in_sec)
30.
31. print(wait_times)
32. print(np.sum(wait_times))
33.
34. led = LED("GPIO14")          #set LED output
35. led.off()                   #clearing outputs to make sure LED is off
36.
37. time.sleep(60)              #setup period 1 minute
38. led.on()
39. print("on")
40. time.sleep(5)               #5sec trial run
41. led.off()
42. print("off")
43.
44.
45. def play_sound(dur, freq):  #defining sound function
46. """
47.     This function passes the stimulation parameters to the
48.     commandline "play" command.
49. """
50.     os.system('play -n synth %s sin %s' %(dur, freq))
51.
52.
53. print("STARTING EXPERIMENT")
```

```
54.  
55. for t in wait_times:  
56.     time.sleep(t)           #inter-stimuli-train waittime  
57.  
58.     #with this setup, stimuli trains are ~17sec long between waittimes  
59.     for beep in range(5):    #beep 5 times  
60.         led.on()  
61.         play_sound(0.35, 600) #0.35sec, 600Hz beep  
62.         led.off()  
63.         time.sleep(3)       #wait 3 sec between beeps  
64.  
65. print("ENDING EXPERIMENT")
```

Code 2. Complete code for inter-stimuli wait time generation and stimulation using the Raspberry Pi.

9.2 Auditory Stimulation Parameter Test

In Figure 30 below, I show the potential number of successful stimulation trials given different wait-time distribution parameters. I simulated this by generating 1000 different samples from the distribution given both parameter choices and then tested how many of those would fall within high-quality times during the already observed recordings, averaged across channels. This gives us an approximation of an expected number of successful stimulation trials.

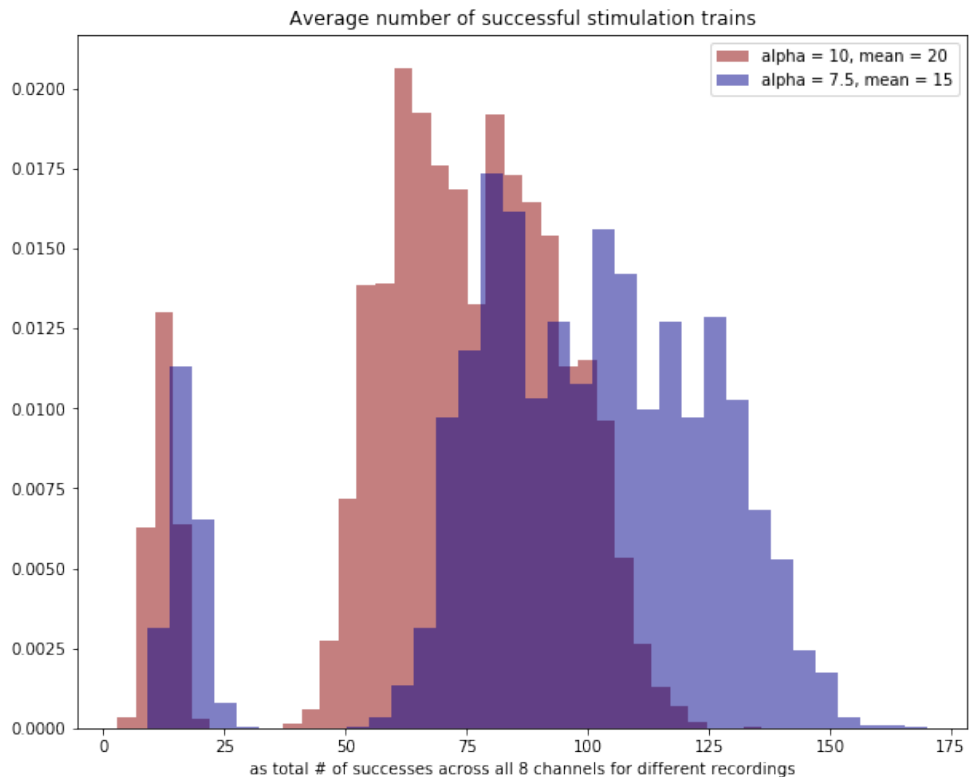


Figure 30. Distribution of expected successful stimulations from wait-time samples generated with two different sets of Gamma parameters. For more details, see the Auditory Stimulation notebook in Appendix 11.3.

9.3 Code Notebooks

All code for this project is presented on my public GitHub repository: <https://github.com/Lyyoness/ALS-Exploratory-Data-Analysis> as well as attached to this project as a zip file.

9.4 IRB

Previously collected data by patient LEK, as well as data collected with the Dreem headset, are covered under ethics approvals by the Ethics Board of the Max Plank Institute. Data collection for the second experiment using auditory stimulation is covered under an ethics proposal by the University of Würzburg.